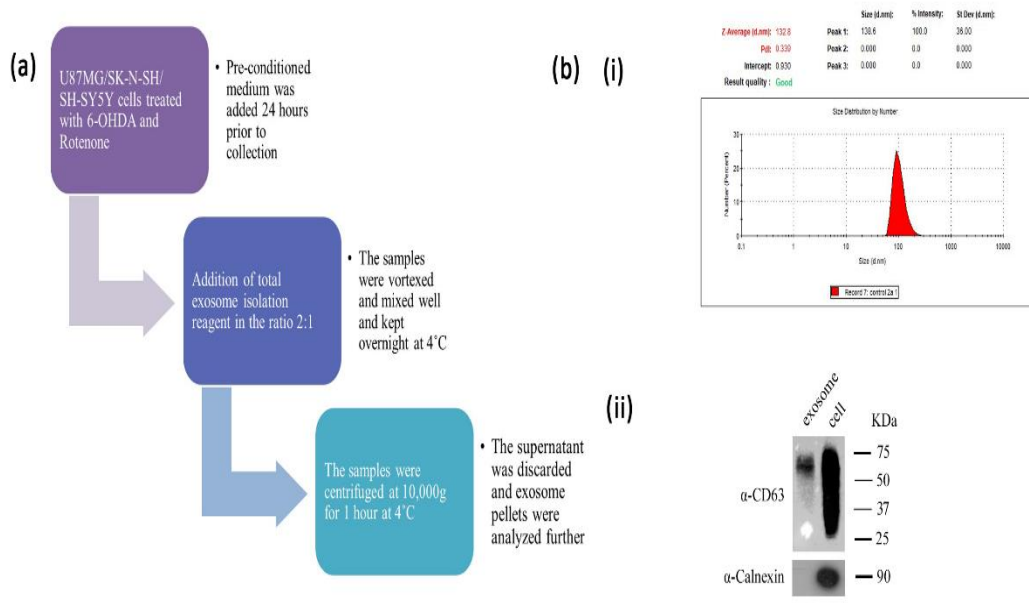


# **Chapter 4. Results & Discussion**

**4.1 – Exosome release is altered in Parkinson's Disease stress conditions and is modulated by the interorganellar crosstalk between mitochondria and lysosome**

**4.1.1 Exosome release is enhanced in Parkinson’s Disease stress conditions**

The exosome release modulation in response to PD stress conditions in different cell types in the brain is not well understood. To achieve this objective, exosomes were isolated from three different cell lines of brain origin, including U-87 MG (likely glioblastoma), SH-SY5Y (neuroblastoma) and SK-N-SH (neuroblastoma; precursor cell line of SH-SY5Y) (Fig 4.1.1(a)). The isolated exosomes were characterized by Nanoparticle Tracking Analysis (NTA) and western blotting. NTA determines the particle size and quantifies the number of particles in a solution by determining its concentration. NTA demonstrated that the size range of the isolated particles from SK-N-SH cells ranges from 80-150nm which is concurrent with the standard size range of exosomes (Fig 4.1.1(b)(i)). Furthermore, western blotting indicated bands of the size ranging from 30-60 KDa for CD63, which is a well-characterized exosome membrane marker. Calnexin, which is an ER-localized protein, was used as a negative control to confirm the purity of the vesicles (Fig 4.1.1(b)(ii)).



**Figure 4.1.1. Isolation and characterization of exosomes:** (a) Schematic flowchart of the exosome isolation (b) Characterization of exosomes by: (i) Nanoparticle Tracking Analysis – U-87 MG exosomes were suspended in DPBS and analyzed by NTA. The exosome size was found to be in a range of 80-150nm. (ii) Western Blotting - Exosomes were isolated from SK-N-SH cells and western blotting was performed and blotted against antibodies as indicated.

To generate PD *in vitro* experimental models, 6-OHDA (6-hydroxydopamine) and rotenone were utilized, which are widely recognized neurotoxins [271], [272], and the exosome release from the cell lines in these PD stress conditions was analyzed. SH-SY5Y cells and U-87 MG cells were treated with 75 $\mu$ M and 0.01 $\mu$ M of 6-OHDA and rotenone respectively, while SK-N-SH cells were treated with 5 $\mu$ M 6-OHDA and 0.1 $\mu$ M rotenone. Since acetylcholine esterase has been described previously to be enriched in exosomes, making it an exosomal marker [273], its enzymatic activity was used to quantify the release of exosomes in PD stress conditions from SH-SY5Y, SK-N-SH and U-87 MG cells. The acetylcholine esterase activity was elevated in the exosomal fractions isolated from the cells in PD stress conditions as compared to untreated (Fig 4.1.2(a)). This was further confirmed by NTA, which demonstrated that the concentration of the exosomal fraction of neuronal as well as glial cells was increased in PD stress conditions (Fig 4.1.2(b)). CD63 levels in 6-OHDA and rotenone conditions were checked in the exosomal fractions by western blotting. Remarkably, increased level of exosomal CD63 was observed in SH-SY5Y, and SK-N-SH neuronal cells and U-87 MG glial cells treated with PD stress inducers as opposed to the control (Fig 4.1.2(c)). All the above results strongly suggested that the exosomal release is enhanced in neuronal as well as glial cells under PD stress conditions.

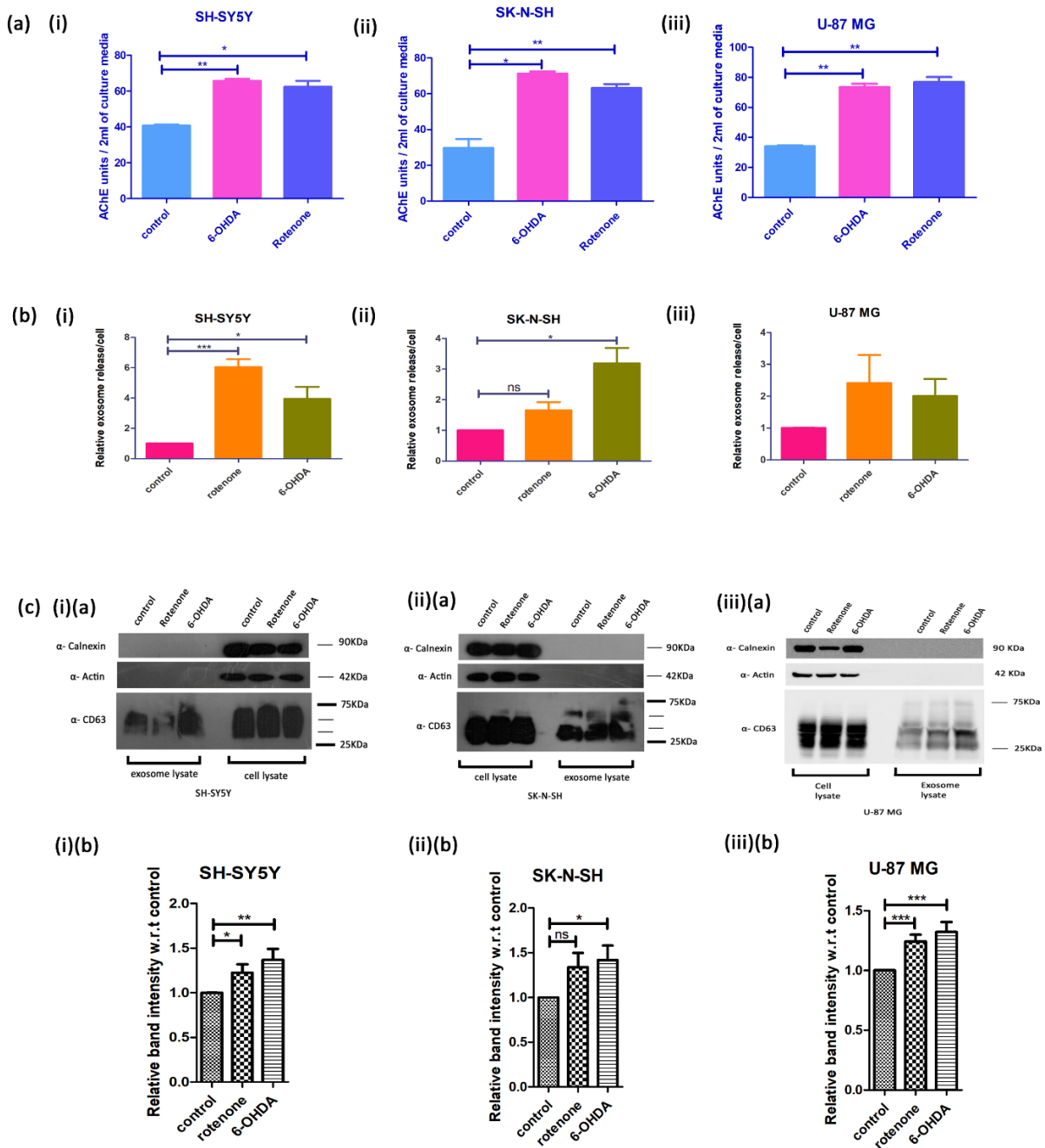


**Figure 4.1.2. Exosome release is enhanced in PD stress conditions:** (a) Exosomes were isolated from (i) SH-SY5Y (ii) SK-N-SH and (iii) U-87 MG cells treated with 6-OHDA and Rotenone and exosome concentration was monitored by acetylcholine esterase activity. Asterisk (\*) and (\*\*) indicates units statistically significant from control; p value <0.05 and <0.01 (respectively), SEM of two independent experiments (b) Exosomes were isolated from (i) SH-SY5Y (ii) SK-N-SH and (iii) U-87 MG cells treated with 6-OHDA and Rotenone and subjected to NTA analysis. Asterisk (\*), and (\*\*\*) indicates levels statistically significant from control; p value <0.05 and <0.001 (respectively), SEM of

three independent experiments (c) Exosomes were isolated from (i)(a) SH-SY5Y (ii)(a) SK-N-SH and (iii)(a) U-87 MG cells treated with 6-OHDA and Rotenone and were subjected to western blot analysis using the indicated antibodies. Relative quantification of CD63 as compared to untreated samples in (i)(b) SH-SY5Y (ii)(b) SK-N-SH and (iii)(b) U-87 MG exosome lysates of cells treated with 6-OHDA and Rotenone. Asterisk (\*), (\*\*), and (\*\*\*) indicates units statistically significant from control; p value <0.05, <0.01 and <0.001 (respectively), SEM of three independent experiments.

### **4.1.2 Parkinson's Disease stress conditions lead to mitochondrial dysfunctions**

Several evidence suggest that mitochondrial morphology, dysfunctions, and oxidative stress generation are the major factors which contribute to the pathogenesis of PD. These factors affect many cellular pathways which can lead to cell death; hence the alteration of mitochondrial functions in PD stress conditions was monitored. Firstly, the mitochondrial morphology of U-87 MG glial cells was observed under PD stress conditions. Confocal microscopy analysis indicated that the untreated cells have an extensive mitochondrial network, whereas the cells treated with 6-OHDA, and rotenone show a fragmented mitochondrial network (Fig 4.1.3(a)). The mitochondrial complex I activity was assessed by spectrophotometric method in neuronal cells under PD stress conditions. Both SH-SY5Y and SK-N-SH show a significant decline in the complex I activity in PD stress conditions (Fig 4.1.3(b)). Further, ATP levels generated in the cells on inducing PD stress conditions were monitored. Neuronal SH-SY5Y and SK-N-SH cells show a decrease in ATP levels in presence of 6-OHDA and rotenone (Fig 4.1.3(c)(i) and (ii)), while U-87MG glial cells also show a remarkable decline (Fig 4.1.3(c)(iii)). All these results collectively suggest that the mitochondrial functions are hampered under PD stress conditions.

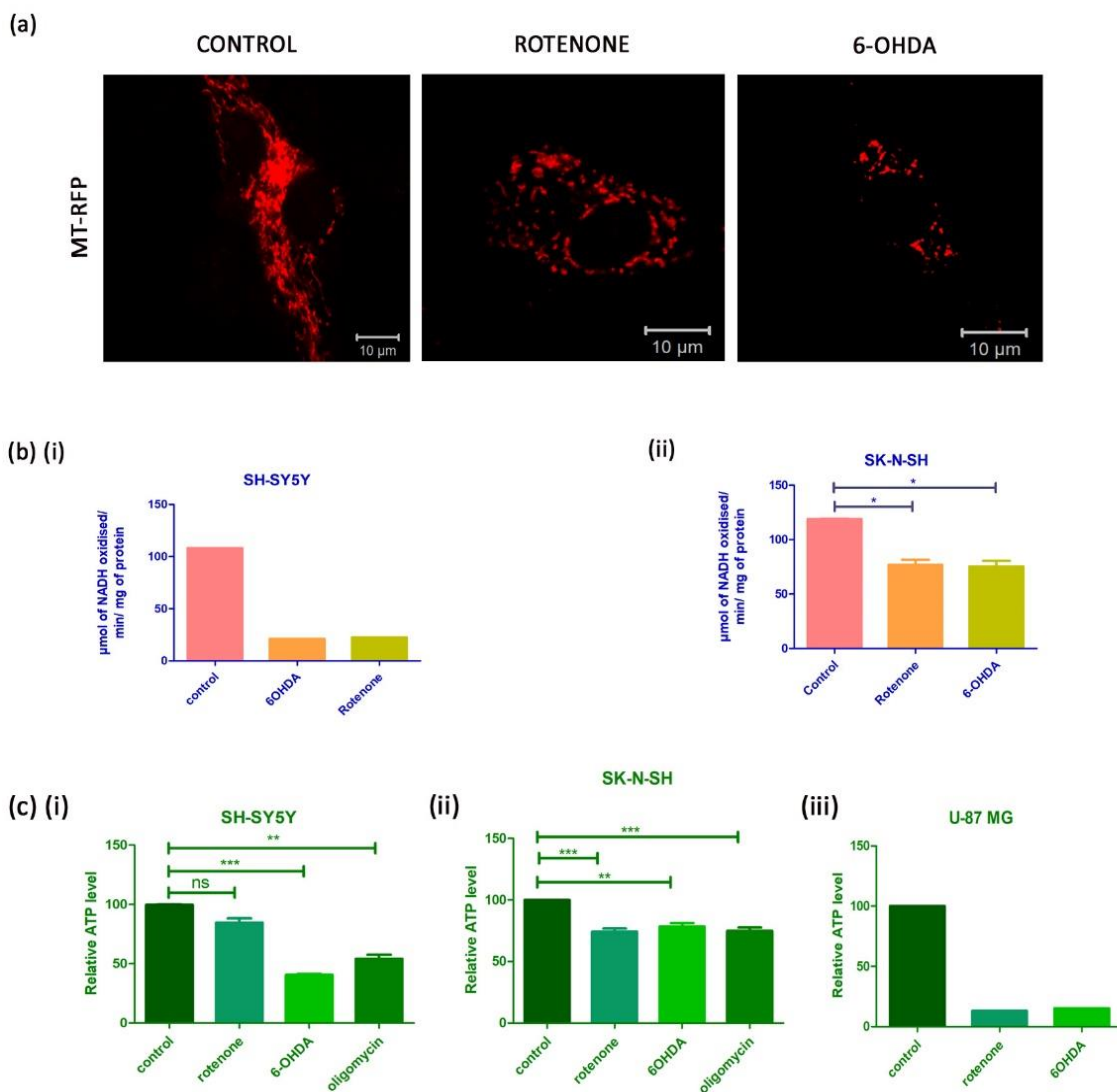


**Figure 4.1.3. PD stress conditions lead to mitochondrial dysfunctions:** (a) MT-RFP transfected U-87 MG cells were treated with 6-OHDA and Rotenone and analyzed by confocal microscopy. (b) (i) SH-SY5Y and (ii) SK-N-SH cells were treated with 6-OHDA and Rotenone and complex I activity was measured by spectrophotometric method. (c) (i) SH-SY5Y (ii) SK-N-SH and (iii) U-87 MG cells were treated with 6-OHDA and Rotenone and ATP levels were determined by luminescence method. Asterisk (\*), (\*\*) and (\*\*\*) indicates levels statistically significant from control; p value <0.05, <0.01 and <0.001 (respectively), SEM of minimum two or three independent experiments.

**4.1.3 Lysosomal functions are altered in Parkinson’s Disease stress conditions**

Emerging evidence suggest that mitochondrial dysfunction and OXPHOS assembly results in a disruption of NADH/NAD ratio, which can also induce lysosomal dysfunctions; indicating that the mitochondrial and lysosomal functions are interlinked, but this mechanism is not clear in PD [274]. Hence, lysosomal functions and their alterations under PD stress conditions were analyzed. The number of lysosomes in neuronal and glial cells under PD stress conditions were observed by confocal microscopy and counted by using LysoTracker blue dye. The number of lysosomes significantly drops in both the neuronal cells as well as glial cells in PD stress conditions (Fig 4.1.4). The decrease in lysosome number is most pronounced in the glial cells as compared to the neuronal cells. Interestingly, SK-N-SH dopaminergic cells overall have a low number of average lysosomes per cell, which is not the case in SH-SY5Y cells where there are numerous lysosomes per cell.

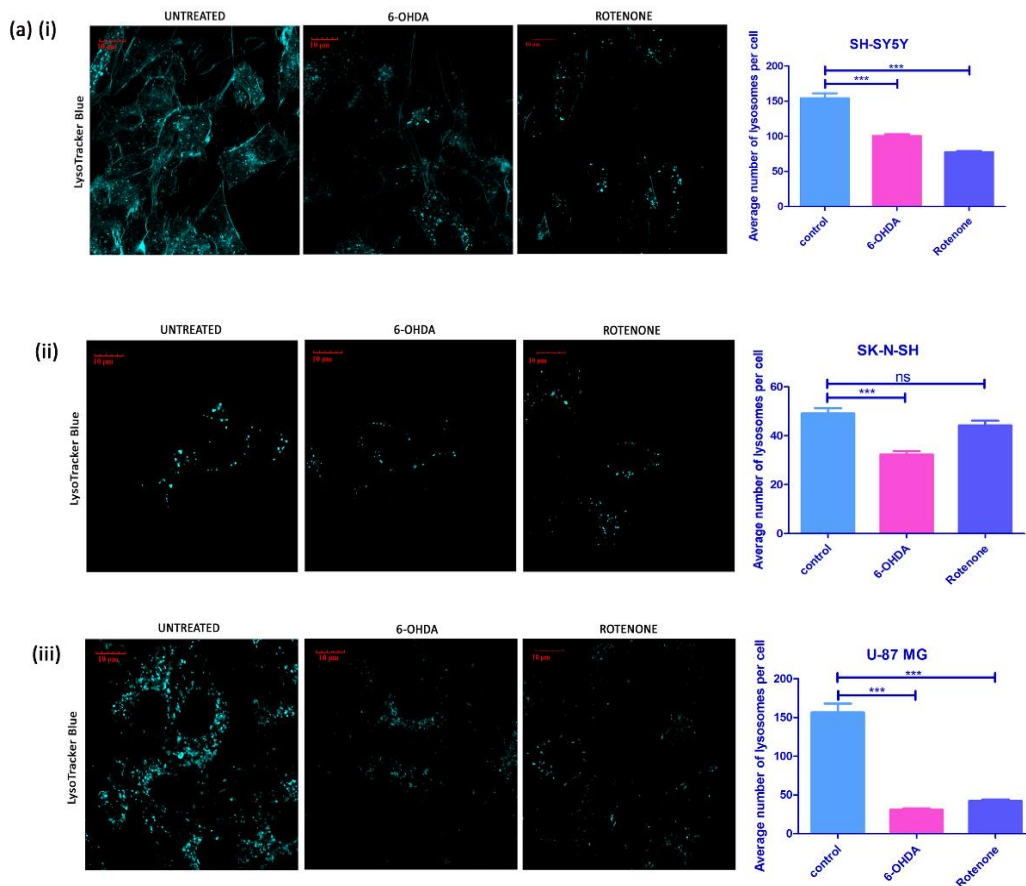


**Figure 4.1.4. The number of lysosomes decline under PD stress conditions:** (a) (i) SH-SY5Y (ii) SK-N-SH and (iii) U-87 MG cells were treated with 6-OHDA for 24h. After treatment cells were stained with LysoTracker Blue as described in method section and was visualized by confocal microscopy. Asterisk (\*\*\*) indicates number of statistically significant from control; p value <0.001(respectively), SEM of minimum two or three independent experiments.

The function of lysosomes is critical for autophagy and hence degradation of  $\alpha$ -syn aggregates and turnover of mitochondria, hence, functional acid phosphatase activity of the lysosomes was performed in neuronal and glial cells under PD stress conditions. Lysosomal acid phosphatase activity was decreased in PD stress conditions, U-87 MG glial cells showed a more compromised lysosomal acid phosphatase activity as compared to both SH-SY5Y and SK-N-SH neuronal cells (Fig 4.1.5(a)). TFEB is a transcription factor and a master regulator of lysosome biogenesis and autophagy, and nuclear translocation of TFEB is essential for activating transcriptional programmes related to lysosomal biogenesis [275]; therefore, the nuclear localization of TFEB was assessed. On using western blotting and TFEB-specific antibody to check the nuclear localization of TFEB in PD stress conditions, a reduced TFEB nuclear localization was observed in both SH-SY5Y neuronal and U-87 MG glial cells in 6-OHDA conditions, although the levels remained unchanged in rotenone stress conditions (Fig 4.1.5(b)). Relative quantification of the western blots confirm that the TFEB/Lamin ratio decreases in 6-OHDA treatment as compared to untreated, and no significant change is observed under Rotenone conditions (Fig 4.1.5(b)).

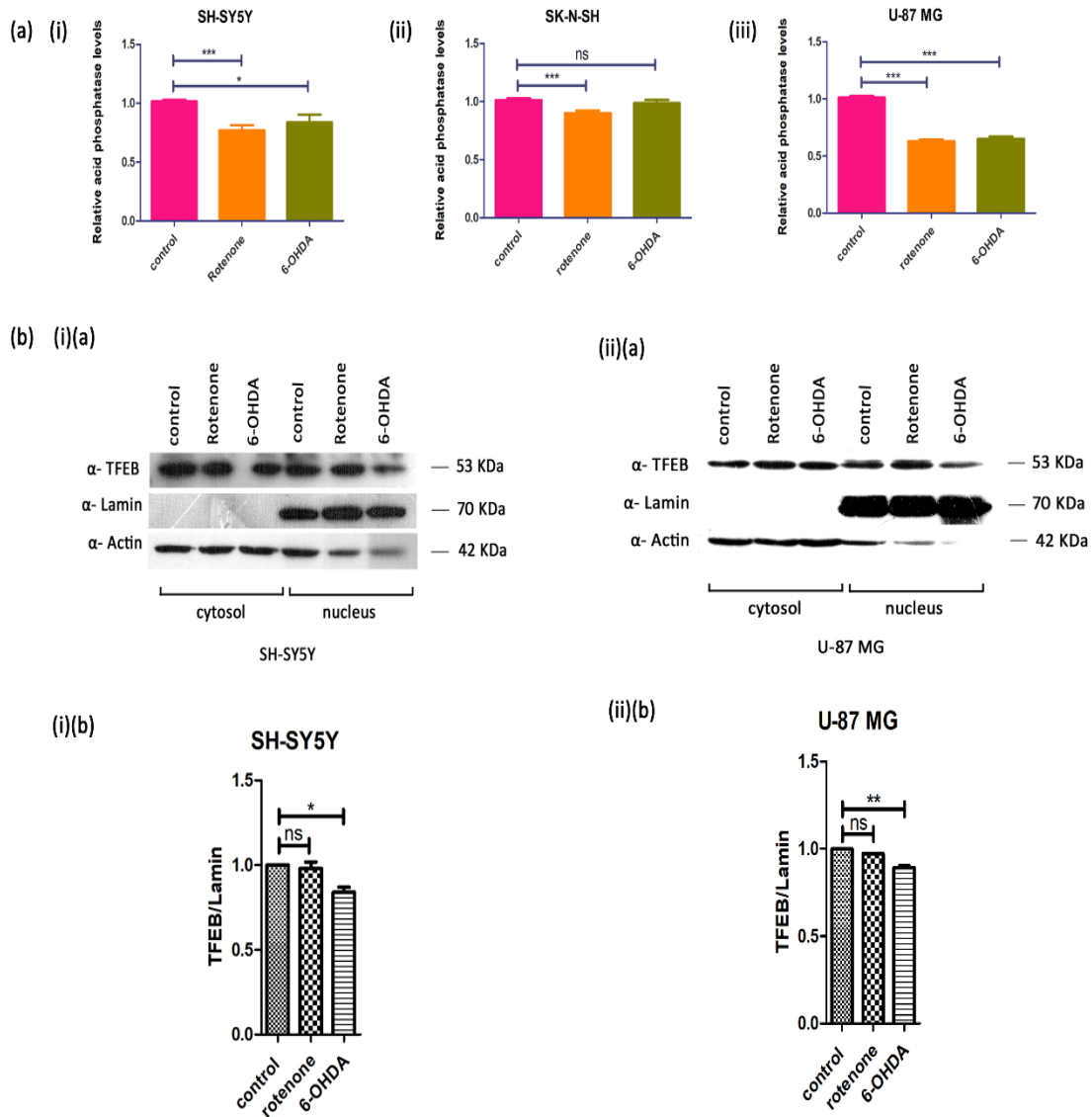


**Figure 4.1.5. Lysosome functions are altered under PD stress conditions:** (a) (i) SH-SY5Y (ii) SK-N-SH and (iii) U-87 MG cells were treated with 6-OHDA and Rotenone for 24h. After treatment, acid phosphatase activity was determined by as described in method section. Asterisk (\*) and (\*\*\*) indicates acid phosphatase levels statistically significant from control; p value <0.05 and <0.001(respectively), SEM of minimum two or three independent experiments. (b) (i) SH-SY5Y and (ii) U-87 MG cells were treated with 6-OHDA and Rotenone and nuclear fractionation was performed and subjected to western blot analysis using the indicated antibodies. Relative quantification of TFEB protein levels in (i)(b) SH-SY5Y and (ii)(b) U-87 MG cells treated with 6-OHDA and Rotenone. Asterisk (\*) and (\*\*\*) indicates units statistically significant from control; p value <0.05 and <0.01 (respectively), SEM of two independent experiments.

### **4.1.4 Altered autophagic flux modulates exosome release in PD stress conditions**

Protein homeostasis is maintained in cells by the process of autophagy, which involves the clearance and degradation of cell contents, and the accumulation of protein aggregates in neurodegeneration is one of the major factors for causing a deficiency in basal autophagy [276]. The final step of autophagy involves fusion with the lysosome, and since the above results suggested that lysosomal dysfunction occurs in PD stress conditions, this could affect overall autophagy as well. Therefore, autophagy flux was monitored in neuronal and glial cells under PD stress conditions using a tandem-mcherry-GFP-LC3 construct. Transfection of all the neuronal and glial cells with the tandem construct was done and subsequently treated with PD stress inducers and observed by confocal microscopy. The yellow-green puncta (red and green merge) indicate autophagosomes whereas red puncta indicate autophagosomes fused with lysosomes also called as autophagolysosomes [277]. In both neuronal and glial cells, the number of red puncta declined in PD stress conditions, while the yellow puncta significantly increased, indicating reduced autophagic flux (Fig 4.1.6(a)). Further, autophagy was examined by monitoring the LC3 levels in PD stress conditions by immunoblotting. LC3 is a well-known autophagy marker; its cytosolic form (LC3-I) gets conjugated to phosphatidylethanolamine to form the LC3-II form, which is eventually recruited to the autophagosome membrane for degradation [278]. In SH-SY5Y neuronal cells, 6-OHDA induces conversion of LC3-I to LC3-II, which is further enhanced on blocking the autophagy with Bafilomycin (100nM) (Fig 4.1.6(b)(i)). Similar results are obtained in SK-N-SH dopaminergic neuronal cells (Fig 4.1.6(b)(ii)). However, a decrease in LC3-II levels is observed in U-87 MG glial cells but LC3 accumulates when co-treated with Bafilomycin A1 (Fig 4.1.6(b)(iii)). These results indicate alteration of autophagic flux under PD stress conditions.

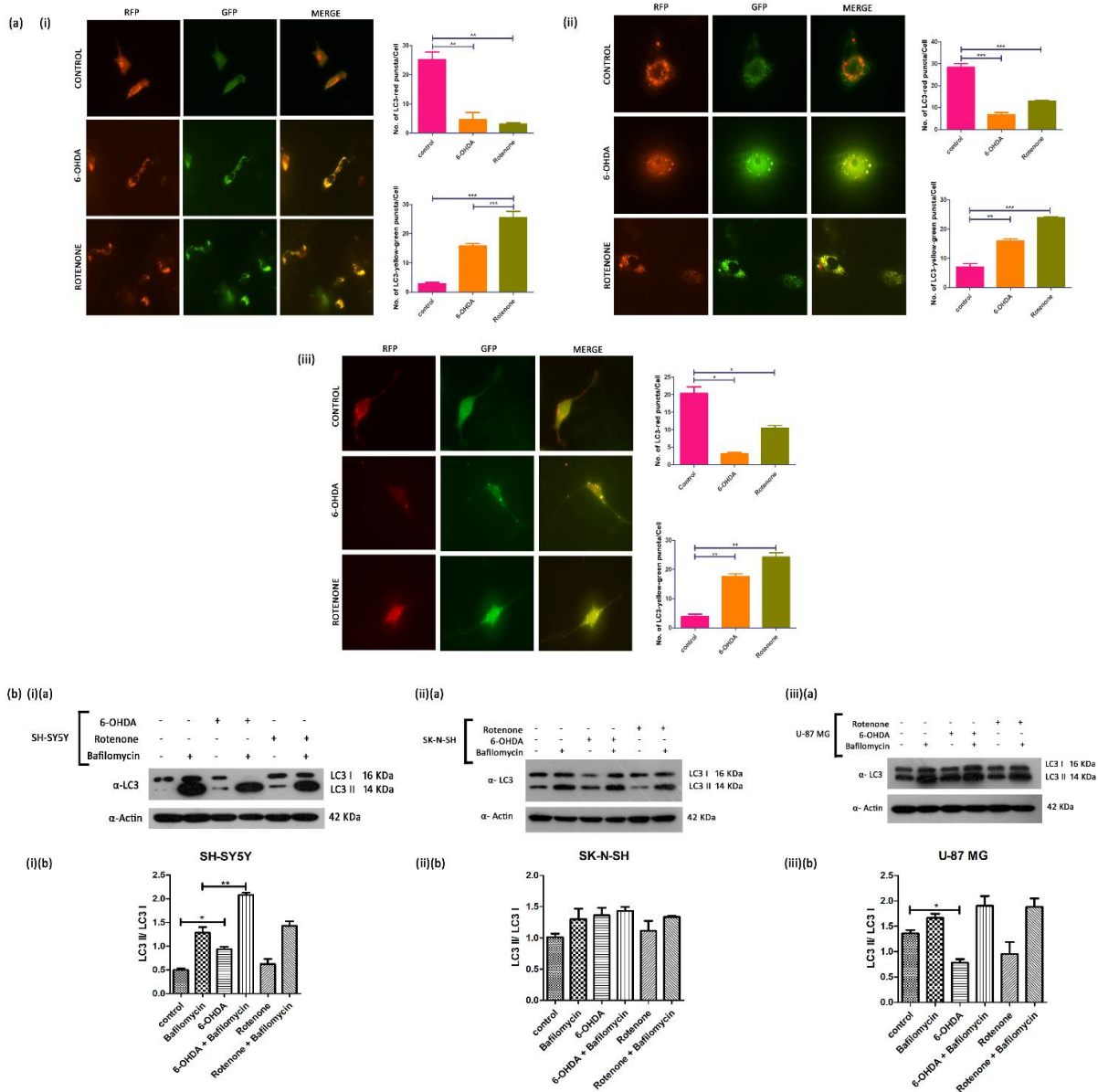


**Figure 4.1.6. Autophagy flux is altered under PD stress conditions:** (a) Quantification of red and green puncta in mCherry-GFP-LC3 transfected cells in the presence and absence of 6-OHDA and Rotenone. The numbers of LC3 puncta per cell were counted and graph was plotted for numbers of mCherry-LC3 puncta per cell in (i) SH-SY5Y (ii) SK-N-SH and (iii) U-87 MG. Asterisk (\*) and (\*\*) and (\*\*\*) indicates number of LC3 puncta statistically significant from control; p value <0.05, <0.01 and <0.001 (respectively), SEM of three independent experiments. (b) (i)(a) SH-SY5Y (ii)(a) SK-N-SH and (iii)(a) U-87 MG cells were treated with Rotenone and 6-OHDA and western blot analysis of autophagy marker, LC3 was performed in presence and absence of Bafilomycin A1. Relative quantification of LC3 II/ LC3 I ratio in (i)(b) SH-SY5Y (ii)(b) SK-N-SH and (iii)(b) U-87 MG cells treated with 6-OHDA and Rotenone in

presence and absence of Bafilomycin A1. Asterisk (\*) and (\*\*) indicates levels statistically significant from control; p value <0.05 and <0.01 (respectively), SEM of three independent experiments.

There are emerging reports which show the intricate crosstalk between exosome release mechanisms and autophagy in the cell. The exosome release may be a cellular mechanism to circumvent the autophagy defect that occurs during pathogenesis, hence there is a close relationship between the two pathways [279]. To explore the crosstalk between the exosome release pathway and autophagy in PD stress conditions; neuronal and glial cells were treated with 6-OHDA and rotenone, and autophagy pathway was inhibited using Bafilomycin, and subsequent exosome release in these conditions was monitored using immunoblotting against CD63. In both neuronal and glial cells, exosome release was enhanced in PD stress conditions, as expected according to the previous results. Interestingly, blocking the autophagy pathway by Bafilomycin also enhanced the exosome release, and this process was even more exacerbated when the cells were co-treated with PD stress inducers and Bafilomycin (Fig 4.1.7).

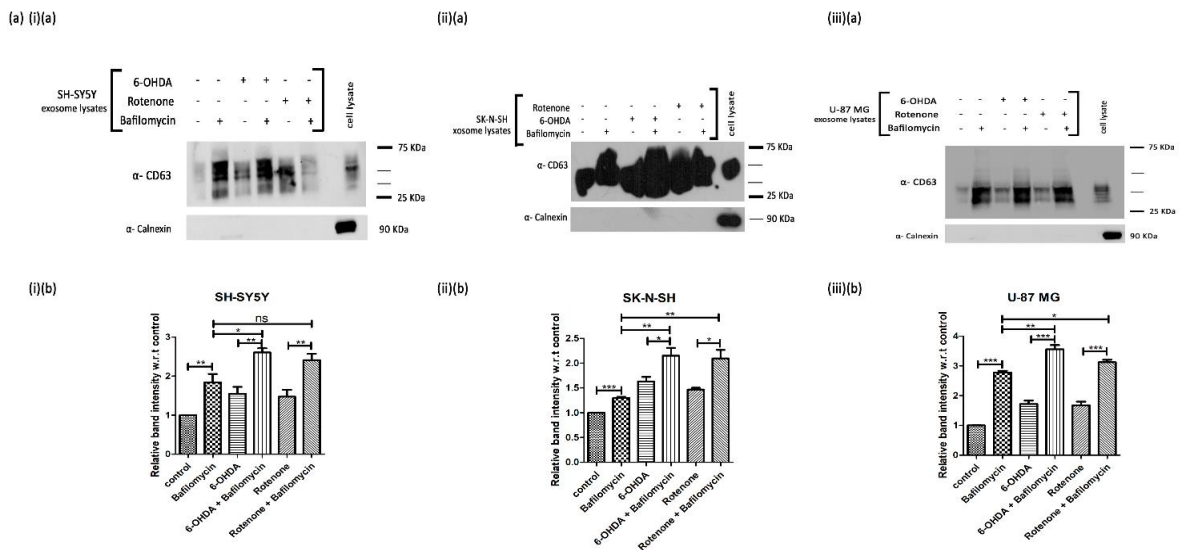


**Figure 4.1.7. Altered autophagic flux modulates exosome release in PD stress conditions:** (a) (i)(a) SH-SY5Y (ii)(a) SK-N-SH and (iii)(a) U-87 MG cells were treated with Rotenone and 6-OHDA and subsequent exosome release was monitored in presence and absence of Bafilomycin A1 by performing western blot against the exosome marker, CD63. Relative quantification of CD63 as compared to untreated samples in (i)(b) SH-SY5Y (ii)(b) SK-N-SH and (iii)(b) U-87 MG exosome lysates of cells treated with 6-OHDA and Rotenone in presence and absence of Bafilomycin

A1. Asterisk (\*), (\*\*) and (\*\*\*) indicates levels statistically significant from control; p value <0.05, <0.01 and <0.001 (respectively), SEM of three independent experiments.

The autophagic flux was also monitored using Wortmannin, which is a widely used autophagy inhibitor. LC3-II accumulates in cells co-treated with 6-OHDA and wortmannin which indicates defect in autophagic flux in SH-SY5Y dopaminergic neuronal cells (Fig 4.1.8(a)). Similarly, subsequent exosome release was checked in SH-SY5Y and SK-N-SH neuronal cells and U-87 MG glial cells under PD stress conditions co-treated with wortmannin. The cells treated with wortmannin did not significantly alter the exosome release in the cells, whereas decreased in cells co-treated with 6-OHDA and Rotenone with wortmannin (Fig 4.1.8(d),(e) and (f)).

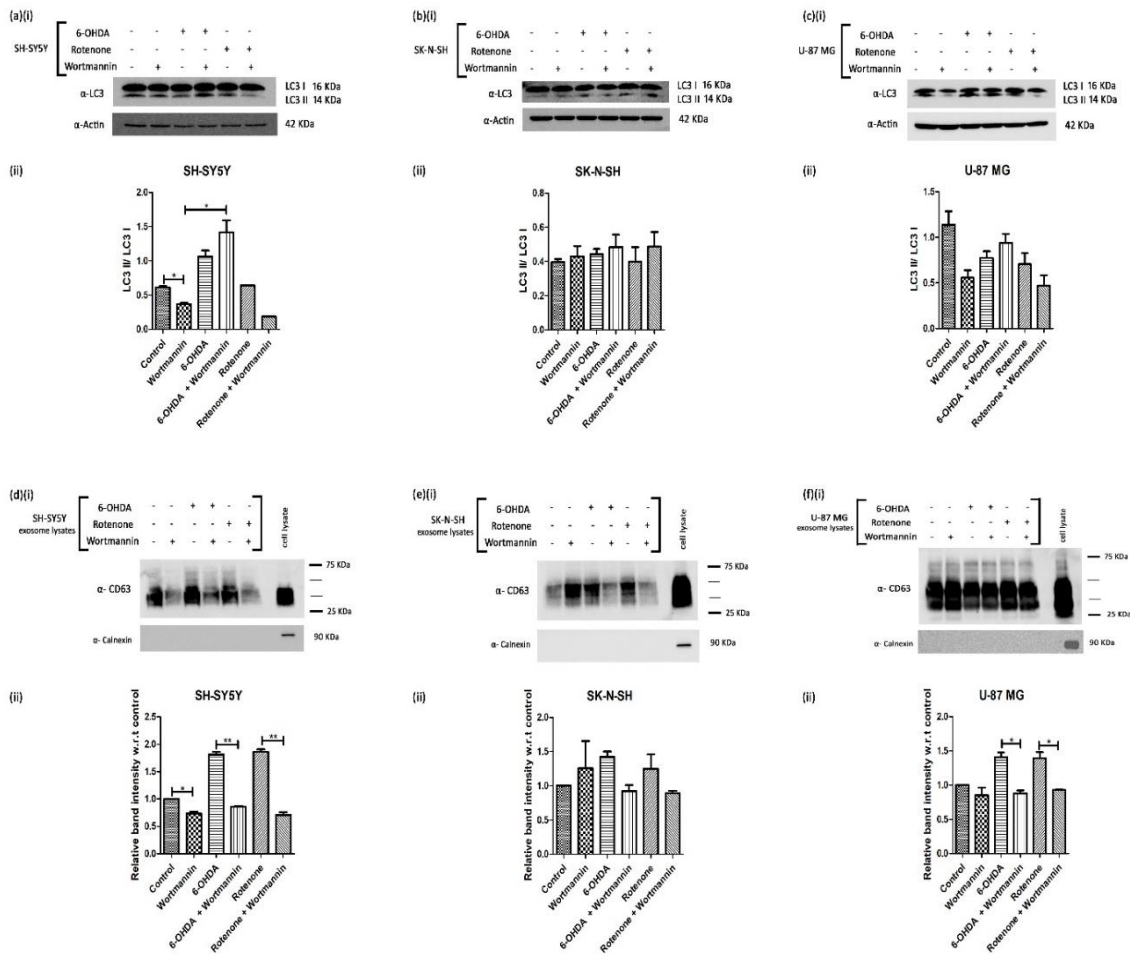


### **Figure 4.1.8. Alteration of autophagic flux by wortmannin decreases exosome release in PD stress conditions:**

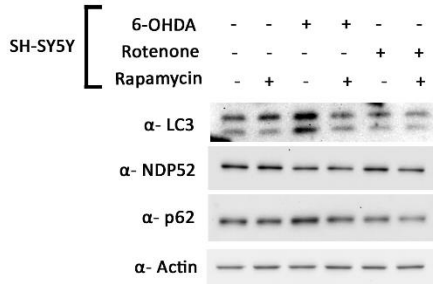
(a)(i) SH-SY5Y (b)(i) SK-N-SH and (c)(i) U-87 MG cells were treated with Rotenone and 6-OHDA and western blot analysis of autophagy marker, LC3 was performed in presence and absence of wortmannin. Relative quantification of LC3 II/ LC3 I ratio in (a)(ii) SH-SY5Y (b)(ii) SK-N-SH and (c)(ii) U-87 MG cells treated with 6-OHDA and Rotenone in presence and absence of wortmannin. Asterisk (\*) indicates levels statistically significant from control; p value <0.05, SEM of two independent experiments. (d)(i) SH-SY5Y (e)(i) SK-N-SH and (f)(i) U-87 MG cells were treated with Rotenone and 6-OHDA and subsequent exosome release was monitored in presence and absence of wortmannin by performing western blot against the exosome marker, CD63. Relative quantification of CD63 as compared to untreated samples in (d)(ii) SH-SY5Y (e)(ii) SK-N-SH and (f)(ii) U-87 MG exosome lysates of cells treated with 6-OHDA and Rotenone in presence and absence of wortmannin. Asterisk (\*) and (\*\*) indicates levels statistically significant from control; p value <0.05 and <0.01 (respectively), SEM of two independent experiments.

### **4.1.5 Enhancement of autophagy flux by rapamycin decreases the release of exosomes in PD stress conditions**

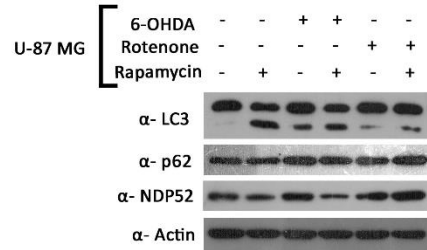
The experiments here showed that mitochondrial and lysosomal dysfunction can modulate the autophagic flux and hence also modulate the exosomal release in PD stress conditions. It was therefore hypothesized that enhancing the basal autophagic flux may decrease the exosomal release. Rapamycin is an allosteric inhibitor of mammalian target of rapamycin (mTOR), and inhibition of mTOR activity enhances autophagy, which in turn plays a role in maintaining metabolic homeostasis [280]; however, its implication in exosomal release in neuronal cells is not well understood. Hence, cells were treated with PD stress conditions in presence and absence of rapamycin and checked for exosome release. Firstly, how rapamycin could modulate the autophagy flux in both neurons and glial cells was checked. SH-SY5Y dopaminergic neuronal cells treated with 6-OHDA showed enhanced level of LC3-II form which decreased when cells were co-treated with rapamycin (Fig 4.1.9(a)(i)). Similarly, enhanced degradation of accumulated LC3-II forms was observed in U-87 MG glial cells (Fig 4.1.9(a)(ii)). This evidence suggested that rapamycin enhances the autophagy flux both in neuronal and glial cells in the presence of PD stress conditions. As enhanced autophagy flux may modulate the release of exosomes, hence, exosomal release was analyzed in presence of PD stress conditions and rapamycin. In SH-SY5Y and U-87 MG cells, the level of CD63 marking the exosome release is enhanced in the presence of 6-OHDA and Rotenone and PD stress conditions. Interestingly, the level of CD63 is decreased in cells co-treated with 6-OHDA and Rotenone with rapamycin both in SH-SY5Y and U-87 MG cells (Fig

4.1.9(b)(i) and (ii)). These experiments suggest that enhancing the autophagy through rapamycin decreased the release of exosome both in neuronal and glial cells.

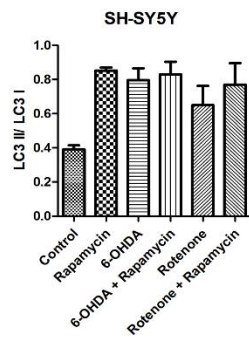
(a) (i) (a)



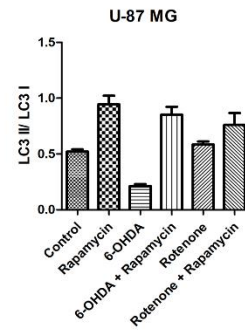
(ii) (a)



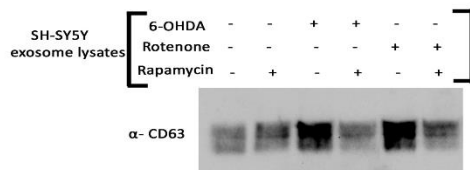
(i) (b)



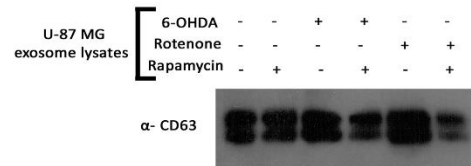
(ii) (b)



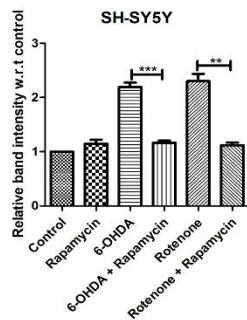
(b) (i) (a)



(ii) (a)



(i) (b)



(ii) (b)

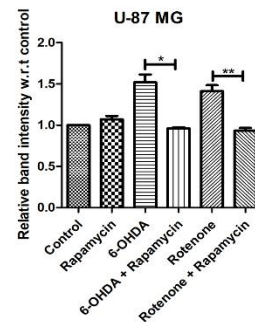


**Figure 4.1.9. Enhancement of autophagy flux by Rapamycin decreases the release of exosomes in PD stress conditions:** (a) (i)(a) SH-SY5Y and (ii)(a) U-87 MG cells were treated with Rotenone and 6-OHDA and western blot analysis of autophagy markers was performed in presence and absence of Rapamycin. Relative quantification of LC3 II/ LC3 I ratio in (i)(b) SH-SY5Y and (ii)(b) U-87 MG cells treated with 6-OHDA and Rotenone in presence and absence of Rapamycin. SEM of three independent experiments. (b) (i)(a) SH-SY5Y and (ii)(a) U-87 MG cells were treated with Rotenone and 6-OHDA and subsequent exosome release was monitored in presence and absence of Rapamycin by performing western blot against the exosome marker, CD63. Relative quantification of CD63 as compared to untreated samples in (i)(b) SH-SY5Y and (ii)(b) U-87 MG exosome lysates of cells treated with 6-OHDA and Rotenone in presence and absence of Rapamycin. Asterisk (\*), (\*\*), and (\*\*\*) indicates levels statistically significant from control; p value <0.05, <0.01 and <0.001 (respectively), SEM of three independent experiments.

### **4.1.6 Discussion**

Parkinson's disease (PD) is typically characterized by the death of dopaminergic neurons in the substantia nigra part of the brain; however, it has been well established that visual impairments occur commonly in PD, along with loss of DA-producing retinal amacrine cells in the inner nuclear and ganglion cell layers and secondary depletion of the dopaminergic fiber plexus of the inner plexiform layer. Similarly, neuronal loss and Lewy body pathology has been observed in the anterior olfactory nucleus as well as the olfactory bulb [281]. The spread of the pathology to different cell types suggests the importance of inter-neuronal communication through exosomes. The exosomal release is a complex crosstalk of mitochondria, lysosome and MVBs to counter the cellular stress and cell may release the damaged organelle/ proteins along with other cargo to protect the cells. In the current study, the mitochondria-lysosomal crosstalk in the release of exosome in PD stress conditions was assessed. Neuronal and glial cell lines were used for the study since it is now well established that glial cells play a role in PD. Glial reaction occurs because of the neuronal cell death in neurodegenerative diseases, and it has been found that even after the initial insult to the neuron has disappeared, the glial reaction initiated further propagates the neuronal degeneration [282], [283]. Moreover, it is now known that the density of microglial cells is remarkably higher in the substantia nigra as compared to the other regions of the brain-like hippocampus and the midbrain regions, which also suggest that the substantia nigra neurons are more susceptible to microglial-mediated injuries, supporting the implication of gliosis in PD pathogenesis [284]. Isolation and characterization of the exosomes released from both cell types was performed. Isolation of exosomes was performed by an affinity purification-based method.

The exosomes were subsequently characterized by Nanoparticle Tracking Analysis and western blotting against the well-characterized exosomal marker, CD63. The exosome release in the presence of 6-OHDA and Rotenone was assessed, which are the two chemicals used to mimic the PD conditions. All the evidence here strongly suggests the enhanced exosomal release in PD stress conditions in dopaminergic neuronal cells (SH-SY5Y and SK-N-SH) and glial cells (U-87 MG).

Previous reports have shown that mitochondria in the neurons are more susceptible to oxidative stress as compared to other cell types [285]. Fragmented mitochondria are usually followed by a decrease in respiration and eventual cell death and is observed in PD models [286]. Mitochondrial fragmentation occurs in the U-87 MG glial cells on treatment with 6-OHDA and Rotenone. Furthermore, consistent with previous reports [119], [287], [288], it was confirmed that SH-SY5Y and SK-N-SH dopaminergic neuronal cells treated with 6-OHDA and Rotenone show impaired mitochondrial complex I activity and ATP level decline and oxidative stress which is the hallmark in PD pathogenesis [289], [290]. An association between PD and hindered complex I activity in the brain was reported by several groups [118], [291]. Chemicals and environmental toxins including Rotenone, 1-methyl-4-phenyl-1,2,3,6-tetrahydropyridine (MPTP), paraquat and nitric oxide are all shown to inhibit mitochondrial functions which show Parkinson-type symptoms [292]. This impaired mitochondrial respiration leads to reduction of ATP levels [288] and is one of the major causes of neurodegeneration, including PD [124].

Mitochondrial OXPHOS activity is known to maintain NADH/NAD ratio which is also important for the maintenance of the lysosomal functions [274]. The crosstalk is further established by recent report where lysosomal dysfunction can lead to generation of a LIPL-4, a lipid signalling messenger which adjust the mitochondrial ETC activity and mitochondrial  $\beta$ -oxidation to reduce lipid storage and promote longevity in *Caenorhabditis elegans* [293]. On the other hand, lysosomes play a vital role in EV biogenesis and its cargo sorting [294]. Furthermore, the large EV release serves as an alternative pathway to eliminate dysfunctional mitochondria when the lysosomal function is compromised [295]. Moreover, a recent study has identified an intracellular hybrid mitochondria-lysosome organelle (MLRO), which is formed by the fusion of mitochondria-derived vesicles (MDVs) with lysosomes and plays a role in regulating overall mitochondria-lysosome homeostasis [296]. Therefore, several emerging reports strongly suggest the mitochondria and lysosomal crosstalk in regulation of homeostasis; however, its implication of

this signalling in PD pathogenesis needs to be further understood. Lysosome is now becoming one of the important organelles in cellular homeostasis. The dysfunction in lysosomes may lead to alteration of several pathways leading to cell death and progression of several chronic diseases. The dysfunction leads to decrease in autophagy flux and hence accumulation of autophagosomes.

The dysfunction in lysosomes in neuronal as well as glial cell lines was shown by using LysoTracker Blue dye and counting average number of lysosomes per cell through confocal microscopy. Acid phosphatase activity was also hampered in PD stress conditions. TFEB is a major regulator in coordinating autophagy induction along with lysosomal biogenesis, and its activation has ameliorated various neurodegenerative disorders in mouse models [297]. By nuclear fractionation of the cells and western blot analysis, it was shown that the nuclear translocation of TFEB is perturbed in 6-OHDA conditions, indicating defective lysosomal biogenesis and autophagy flux.

Recent studies show that autophagy is linked to healthy mitochondrial functioning. Autophagy-deficient fibroblasts decrease the mitochondrial membrane potential by depleting NAD levels. Further, boosting the levels of NAD and maintaining NAD levels protects cell loss even in absence of functional autophagy [298]. Hence, the autophagy flux was monitored in neuronal and glial cells in 6-OHDA and Rotenone conditions using the tandem construct mCherry-GFP-LC3. The number of yellow puncta considerably increased in 6-OHDA and Rotenone conditions indicating the reduced autophagic flux and impaired autophagy. How the impairment of autophagy in PD stress conditions affects the exosome release is not well understood. Hence, the exosome release was assessed under the same conditions. The blocking of autophagy pathway by Bafilomycin A1 greatly enhances the exosome release in the dopaminergic neuronal and glial cells. A recent study has shown that the exosomal cargo (miRNAs) play a role in enhancing the autophagy flux, modulating lysosomal functions and ROS levels under PD stress conditions, which might be a rescue mechanism of the source cell for the bystander cells, and the transfer of the miRNA to recipient cell alleviates mitochondrial ROS levels and cell death [299]. Similarly, another exosomal miRNA is reported to improve the autophagic flux in hepatocytes by increasing TFEB levels in the cell, hereby mediating autophagy repairment [300].

The class III PI3Ks are known to play a role in recruitment of specific effector proteins to promote endocytosis, endosome fusion, and maturation, as well as cargo sorting to lysosomes, and

moreover are essential for the ILV formation [301]. The data here exhibited that inhibition of class III PI3Ks with the help of wortmannin resulted in decreased release of exosomes in PD stress conditions. This indicates that the regulation of exosome release is largely dependent on the inhibition of the autophagy process at the terminal step of fusion of the autophagosome with the lysosome. The results here suggest that wortmannin, which blocks autophagy at the initiation stage, also may affect several other different pathways because of their broad-spectrum action, and hence the enhanced exosome release is not observed in these cases.

The enhancement of autophagy by rapamycin in PD stress conditions in both SH-SY5Y dopaminergic neuronal cells and U-87 MG glial cells showed a decrease in the release of exosomes. This is in consonance with previous reports where it has been observed that rapamycin plays a protective role against cell death in in vitro and in vivo models of PD [280], and this may be because of preventing the exosomal release by enhancing the autophagy flux. This suggests that enhancement of autophagy pathway by Rapamycin could lower the exosome release content by the cells in PD stress conditions, which could provide a therapeutic possibility to stop the spread of the pathogenesis of the disease through exosomes.

**4.2 – Neuronal exosomal miRNAs  
modulate mitochondrial functions and  
cell death in bystander cells**

### **4.2.1 PD-stressed exosomes are internalized by bystander neuronal cells and localize to mitochondria**

Emerging studies suggest that exosomes can mediate inter-neuronal and neuron-glia communication in the brain [302]. To investigate the exosomal crosstalk between different cell types in the brain, exosomes isolated from U-87 MG glial cells and SH-SY5Y dopaminergic neuronal cells were incubated with SK-N-SH (neuronal) cells, and their uptake was observed by confocal microscopy. Different stains selective for RNA and the exosomal membrane were used to track the uptake of exosomes in recipient cells. U-87MG exosomes stained with 1X PKH26 lipophilic dye (to label the exosomal membrane) were incubated with SK-N-SH cells, and the cells were analyzed by confocal microscopy. The red fluorescence inside the cells showed the uptake of exosomes by the recipient cells (Fig 4.2.1(a)(i)). Further, exosomes isolated from SH-SY5Y cells were stained with SYTO RNASelect (for staining RNA) and incubated with SK-N-SH cells. Green-fluorescent labelled exosomal cargo (RNA) was visualized in SK-N-SH cells by confocal microscopy (Fig 4.2.1(a)(ii)). Next, exosomes isolated from SH-SY5Y neuronal cells were stained with two dyes together, SYTO RNASelect and BODIPY TR Ceramide (for staining the exosomal membrane) and incubated with SK-N-SH cells. Merged image shows that the exosomes enter the recipient cells as intact vesicles (Fig 4.2.1(a)(iii)). These experiments clearly indicated that neuron-glia communication takes place via exosomes, which are internalized by the recipient cells as intact vesicles.

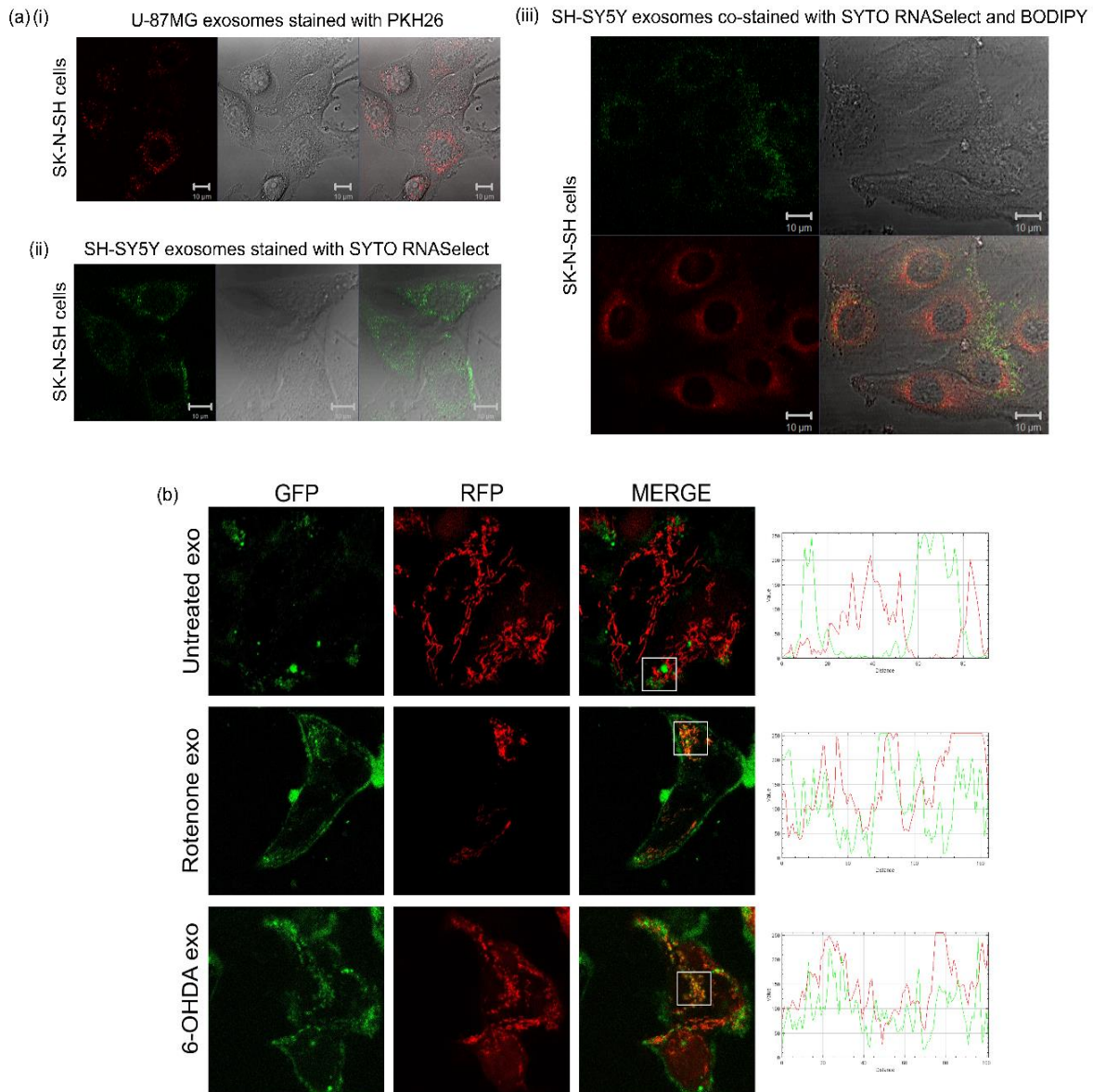


**Figure 4.2.1. Neuronal and glial exosomes are internalized by recipient cells and localize to the mitochondria:**

(a) (i) U-87MG glial exosomes were stained with the exosomal membrane dye PKH26 and incubated with SK-N-SH neuronal cells. (ii) SH-SY5Y exosomes stained for their RNA cargo with SYTO RNASelect were incubated with SK-N-SH cells. (iii) SH-SY5Y exosomes stained with SYTO RNASelect (green) and the exosomal membrane dye BODIPY (red) were incubated with SK-N-SH cells (Scale bar represents 10 $\mu$ m). (b) PD-stressed neuronal exosomes (6-OHDA-exo and rotenone-exo) were incubated with healthy SH-SY5Y neuronal cells expressing the mitochondrial fluorescent protein MT-RFP, and their uptake and localisation were observed by live confocal microscopy. The boxed regions in the merged pictures show the site of co-localization of exosomes with mitochondria, and a correlation plot was generated using ImageJ software. A total of 10 cells were monitored over a period of 2 minutes and three biological replicates of the experiment were performed.

Subcellular localisation and the functional effect of the exosomes upon uptake in the recipient cells was further assessed. SH-SY5Y neuronal cells were treated with the PD stress inducers, 6-OHDA and rotenone, and exosomes isolated from the treated cells (referred to as 6-OHDA-exo and rotenone-exo, respectively, or sometimes collectively as PD-exo) were incubated with healthy bystander SH-SY5Y neuronal cells (Fig 4.2.2). Analysis by confocal microscopy indicated that 6-OHDA-exo and rotenone-exo localize to mitochondria in recipient neuronal cells expressing the mitochondrial fluorescent protein MT-RFP (Fig.1b). The degree of colocalization is higher in the case of 6-OHDA- and rotenone-exo as compared to exosomes from untreated cells (Fig.1b).

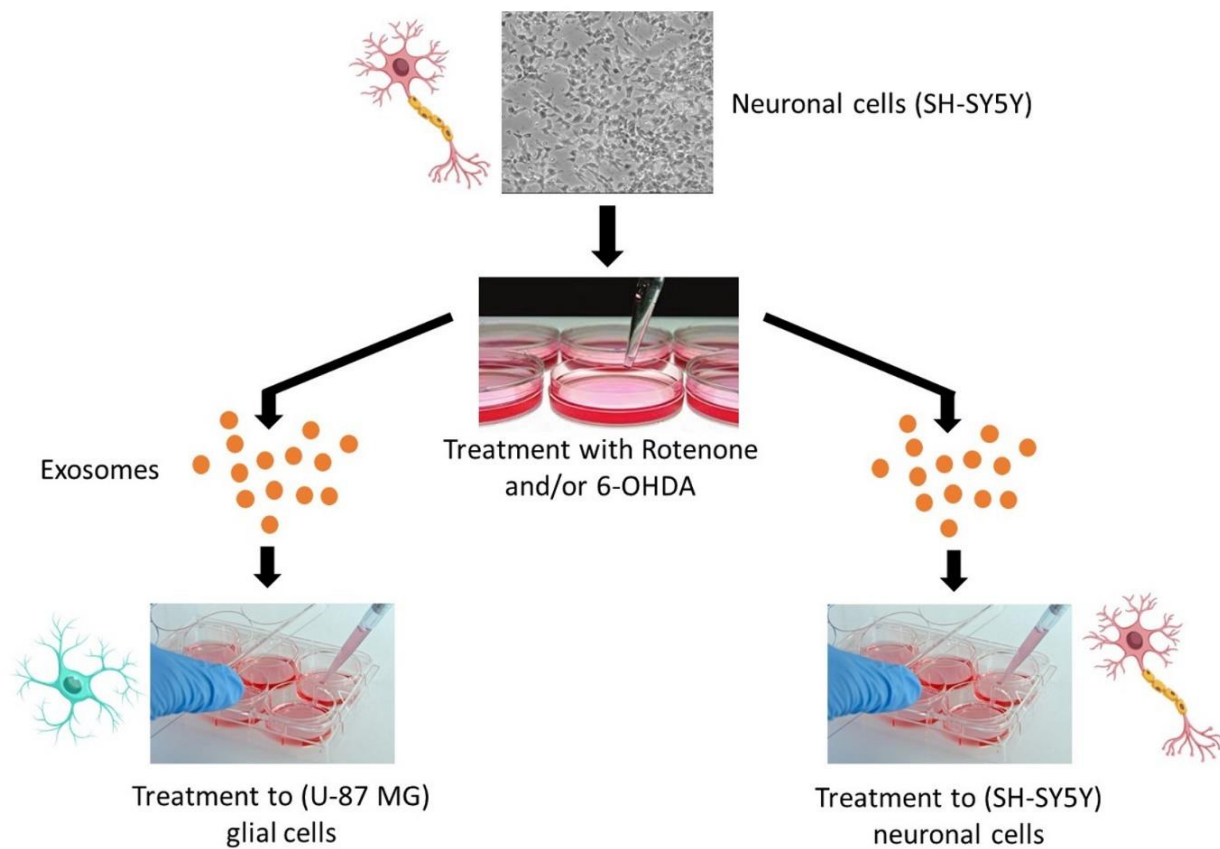


**Figure 4.2.2. Schematic flowchart showing isolation of PD-stressed exosomes from SH-SY5Y neuronal cells and treatment to bystander neuronal cells.**

### **4.2.2 PD-stressed exosomes alter the mitochondrial functions and induces cell death**

Above data suggested that PD-stressed exosomes have an increased localization to mitochondria in recipient cells. It was hypothesized that the exosomal cargo could alter mitochondrial functions, thereby sensitizing neuronal cells to stress-induced cell death. To study the effect of exosomes on mitochondrial functions, SH-SY5Y neuronal cells were treated with 6-OHDA and rotenone, the exosomes isolated from the treated cells (PD-exo) were incubated with healthy bystander SH-SY5Y neuronal cells and U-87 MG glial cells, and mitochondrial ROS levels were determined. Analysis indicated that PD-exo increases mitochondrial ROS levels in the recipient neuronal cells (Fig 4.2.3(a)). Rotenone-treated SH-SY5Y cells were used as a positive control for the study. Total cellular ROS levels were further examined and found that PD-exo increased ROS levels in recipient SH-SY5Y cells at 24h (Fig 4.2.3(b)), using H<sub>2</sub>O<sub>2</sub>-treated cells as a positive control. Similarly, TMRM staining indicated that 6-OHDA-exo, but not Rotenone-exo, reduces the mitochondrial membrane potential in bystander SH-SY5Y cells at 24h (Fig 4.2.3(c)). The results indicate that mitochondrial functions are overall compromised on the incubation of PD-exo with recipient neuronal cells. Similarly, when PD-exo was incubated with healthy U-87 MG glial cells, the mitochondrial ROS levels were elevated (Fig 4.2.4(a)). Moreover, like neuronal recipient cells, the glial cells also showed increased total cellular ROS levels, but this was detected at 48h, and not 24h (Fig 4.2.4(b)). Similarly, TMRM staining indicated that the PD-exo reduces the mitochondrial membrane potential in bystander U-87 MG cells at 48h (Fig 4.2.4(c)).

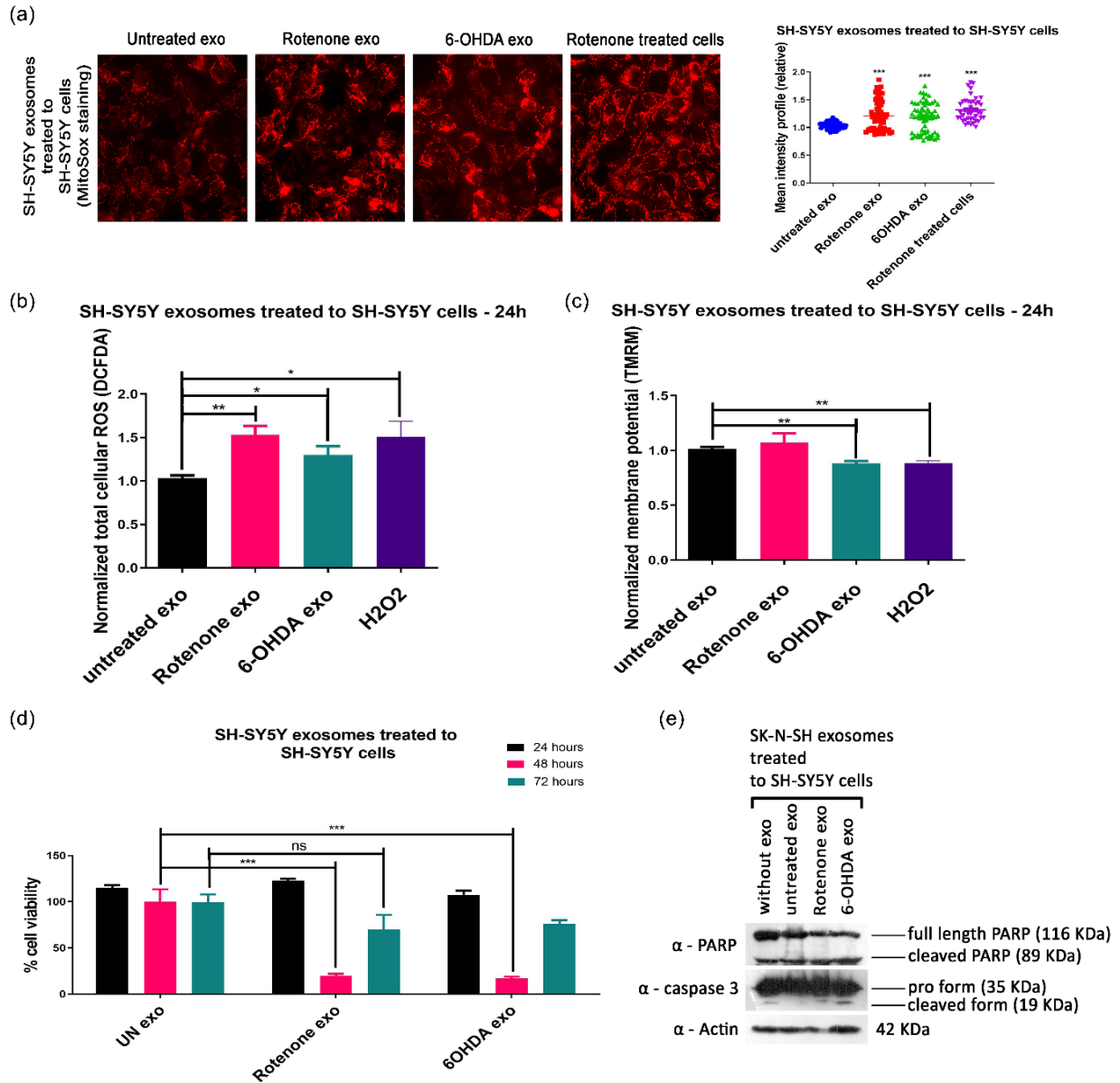


**Figure 4.2.3. PD-stressed neuronal exosomes modulate mitochondrial functions in recipient neuronal cells leading to cell death:** (a) Rotenone-exo, 6-OHDA-exo, or exosomes from untreated cells were incubated with SH-SY5Y neuronal cells for 24 hours, and MitoSox™ levels were analyzed by fluorescence microscopy, using rotenone treated cells as positive control. (b) Exosomes were incubated as indicated above in (a), and total cellular ROS levels were analyzed fluorometrically by H<sub>2</sub>DCFDA staining, using H<sub>2</sub>O<sub>2</sub> treated cells as positive control. (c) Exosomes were incubated as indicated above in (a), and the mitochondrial membrane potential was determined fluorometrically by using TMRM stain, using H<sub>2</sub>O<sub>2</sub> treated cells as positive control. (d) Exosomes as described above were incubated with SH-SY5Y neuronal cells for the indicated time periods, and cellular viability was determined by MTT assay. Asterisk (\*), (\*\*), and (\*\*\*) indicates values statistically significant from control; p value <0.05, <0.01, and <0.001 (respectively), SEM of three or four independent experiments.

Since mitochondrial ROS are known to lead to cytotoxicity [303], hence neuronal cell death was analyzed upon treatment with PD-exo. MTT assay indicated that significant loss of cell viability is observed after 48h and 72h post-treatment of PD-exo in SH-SY5Y cells as well as U-87 MG cells (Fig 4.2.3(d) and Fig 4.2.4(d)). The results suggest that exosomes released from PD-stressed cells can be actively internalized by bystander neuronal or glial cells, localise to mitochondria, altering its functions and leading to cell death. Further, exosomes derived from SK-N-SH PD-stressed neuronal cells were incubated with healthy bystander SH-SY5Y neuronal cells, and levels of cell death markers, PARP and caspase-3 were analyzed by western blotting. The 89 kDa band indicating cleaved PARP was increased, and the pro-form of PARP at 116 kDa was decreased in the cells treated with the PD-exosomes. This was accompanied by the increased levels of cleaved caspase-3 as well (Fig 4.2.3(e)). These results suggested that PD-exo, when internalized in recipient neuronal and glial cells, probably localize to the mitochondria, and alter its functions, leading to loss in cell viability mediated by apoptosis.

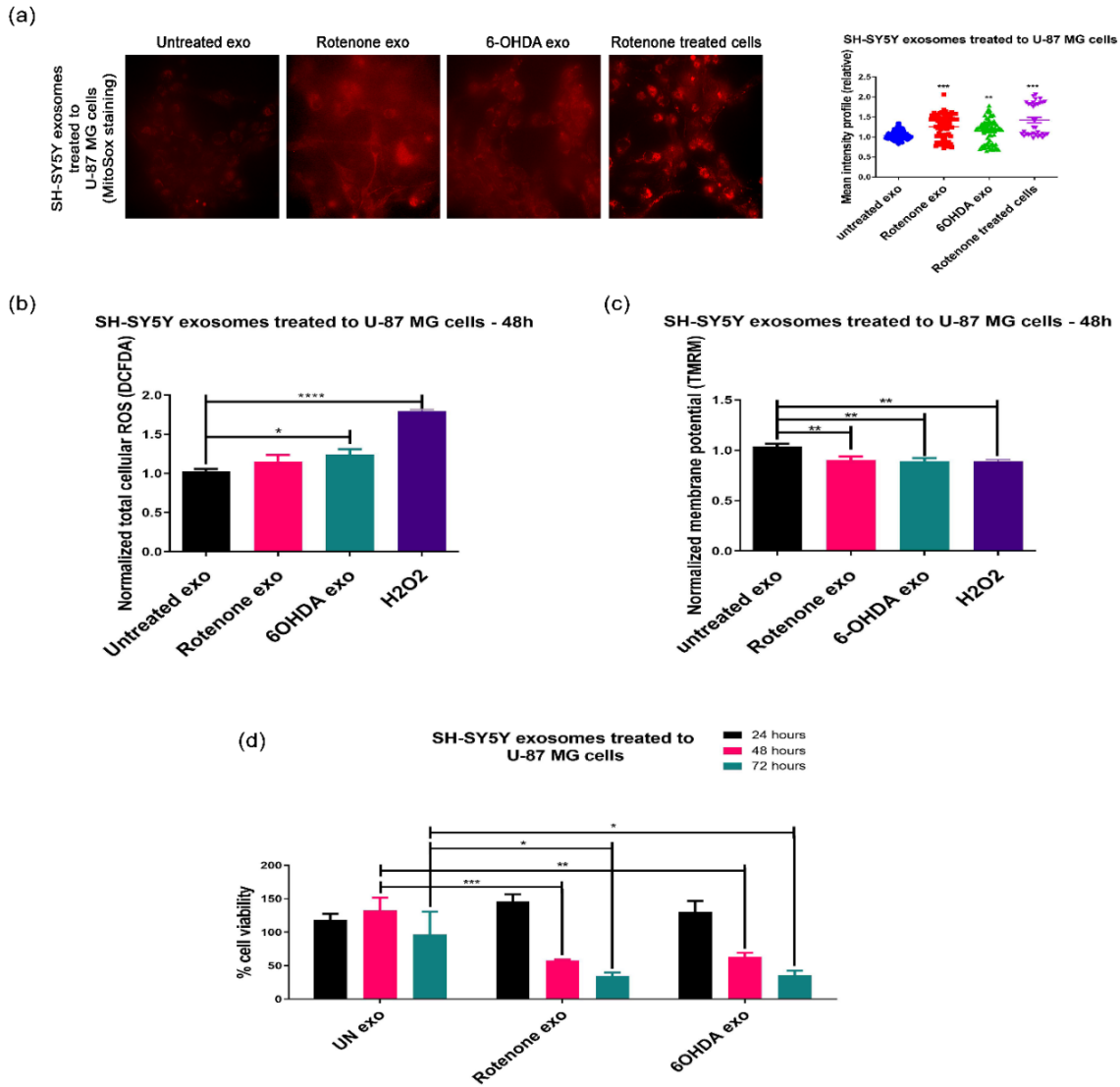


**Figure 4.2.4. PD-stressed neuronal exosomes modulate mitochondrial functions in recipient glial cells leading to cell death:** (a) Rotenone-exo, 6-OHDA-exo, or exosomes from untreated cells were incubated with U-87 MG glial cells for 24 hours, and MitoSox™ levels were analyzed by fluorescence microscopy, using rotenone treated cells as positive control. (b) Exosomes were incubated as indicated above in (a), and total cellular ROS levels were analyzed fluorometrically by H<sub>2</sub>DCFDA staining, using H<sub>2</sub>O<sub>2</sub> treated cells as positive control. (c) Exosomes were incubated as indicated above in (a), and the mitochondrial membrane potential was determined fluorometrically by using TMRM stain, using H<sub>2</sub>O<sub>2</sub> treated cells as positive control. (d) Exosomes as described above were incubated with U-87 MG glial cells for the indicated time periods, and cellular viability was determined by MTT assay. Asterisk (\*), (\*\*), (\*\*\*) and (\*\*\*\*) indicates values statistically significant from control; p value <0.05, <0.01, <0.001 and <0.0001 (respectively), SEM of three or four independent experiments.

### 4.2.3 PD stress conditions induce differential enrichment of miRNAs in neuronal exosomes

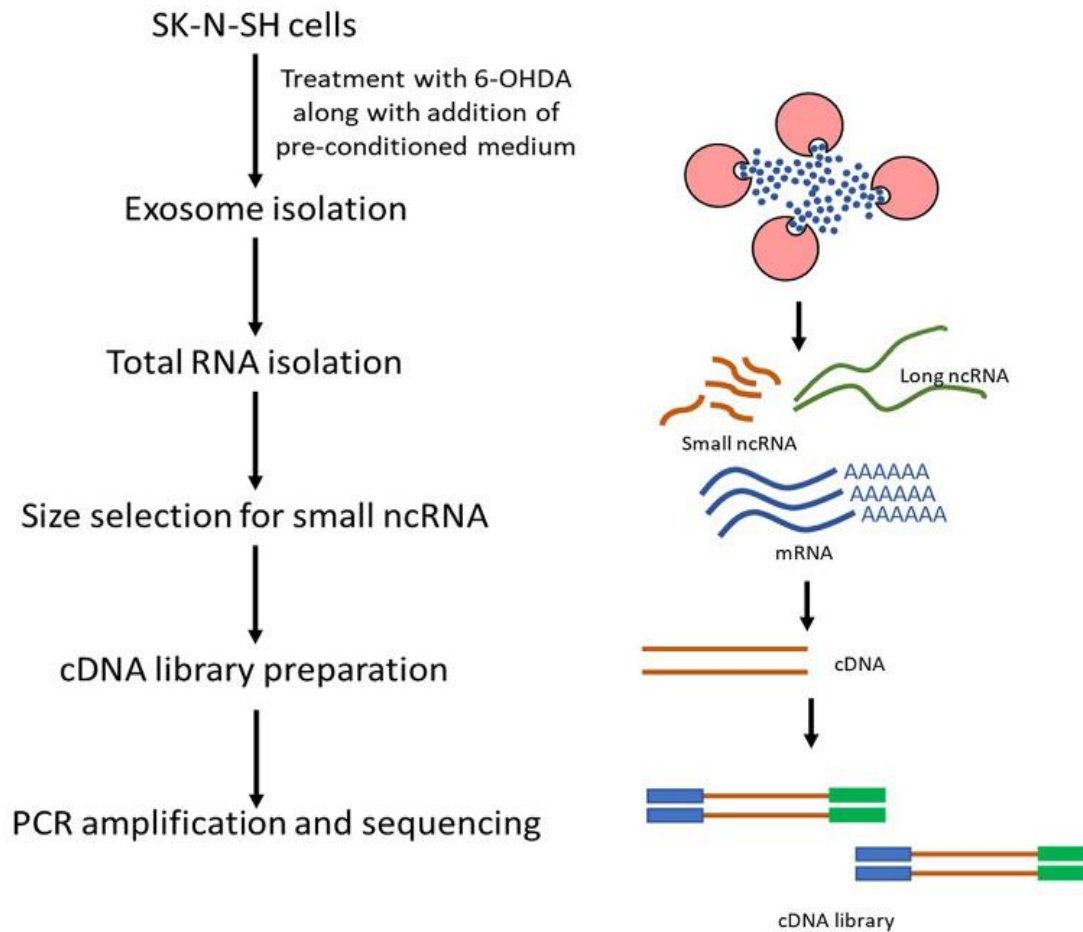
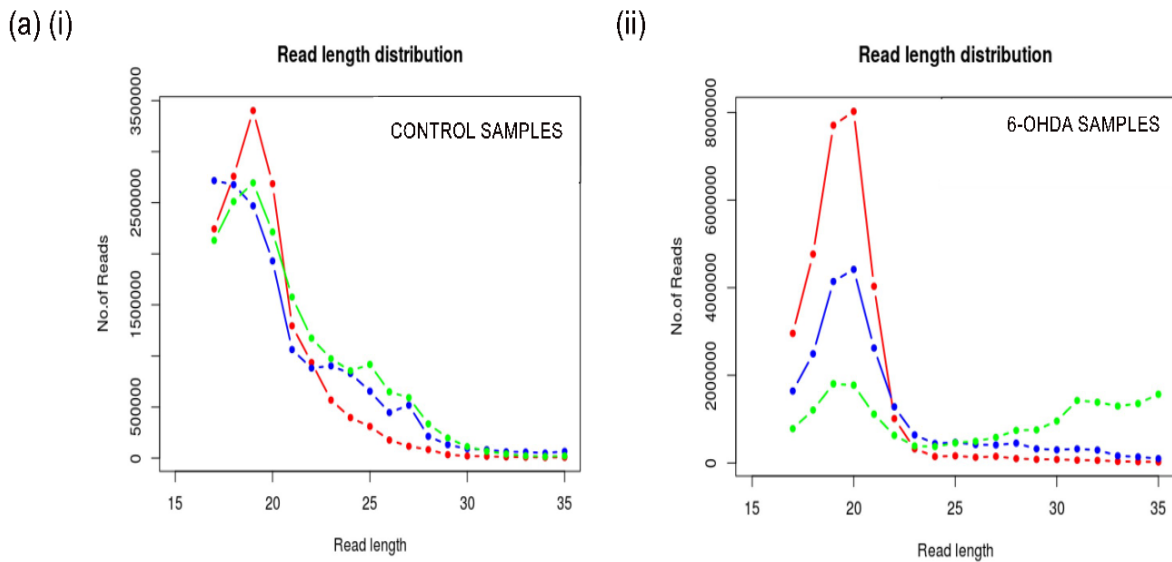


**Figure 4.2.5. Schematic flowchart showing NGS analysis of exosomal RNA of SK-N-SH neuronal cells treated with 6-OHDA.**

Exosomal miRNA profiles from distinct cell types are different, suggesting that an active sorting mechanism exists for the selective enrichment of miRNAs in exosomes [304]. However, the exosomal miRNA profile of dopaminergic neuronal cells under the 6-OHDA-induced PD stress condition has not been systematically explored. SK-N-SH neuronal cells were treated with 6-OHDA and exosomal RNA was analyzed obtained from these cells by NGS (Fig 4.2.5). We observed a difference in the miRNA read length distributions for the different samples. Control

exosomal RNA showed a uniform nucleotide length lying between 18-22nt, whereas 6-OHDA exosomal RNA had a variable nucleotide length indicating a range more than 22nt (Fig 4.2.6(a)). The miRNAs showing upregulated and downregulated levels in exosomes under PD stress conditions were sorted according to their read counts (Fig 4.2.7(c) and (d)). miRNAs were categorized in three different groups: read count of <100, 100-1000, and >1000 (Fig 4.2.6(b)). Downregulated exosomal miRNAs, including miR-181c-5p and miR-155-5p, and upregulated miRNAs, including miR-664b-5p, had low read counts of <100 (Fig 4.2.6(b)). miRNAs like miR-30a-5p, miR-122-5p, miR-320d (100-1000) were comparatively abundant, and three miRNAs, miR-1246, miR-92a-1-5p, and miR-92a-2-5p, were most abundant, with read counts more than 1000 (Fig 4.2.6(b)).



(b)

Read Count of miRNAs	Upregulated miRNAs	Downregulated miRNAs
0-100	hsa-miR-30b-5p, hsa-miR-574-5p, hsa-miR-338-5p, hsa-miR-664b-5p, hsa-miR-484	hsa-miR-1-5p, hsa-miR-181c-5p, hsa-miR-222-5p, hsa-miR-1-3p, hsa-miR-374a-5p, hsa-miR-155-5p
100-1000	hsa-miR-708-5p, hsa-miR-532-5p, hsa-miR-320d	hsa-miR-30a-5p, hsa-miR-122-5p, hsa-miR-93-5p
Above 1000	hsa-miR-92a-1-5p, hsa-miR-92a-2-5p	hsa-miR-1246

**Figure 4.2.6. Read length of miRNAs in NGS and sorting according to read counts:** (a) Read length distribution of miRNAs in (i) control exosome samples and (ii) 6-OHDA exosome samples. (b) miRNAs that were upregulated and downregulated in exosomes in PD-stress conditions were sorted according to their read counts.

NGS data indicated around 170 miRNAs differentially enriched in exosomes from 6-OHDA treated neuronal cells. The heat map shows the log<sub>2</sub>fold change (treatment/control) of some of the notable miRNAs listed in the NGS data that were differentially enriched in exosomes (Fig 4.2.7(a)). NGS analysis showed specific differential enrichment of miRNAs in exosomes under PD stress conditions (Fig 4.2.7(b)).

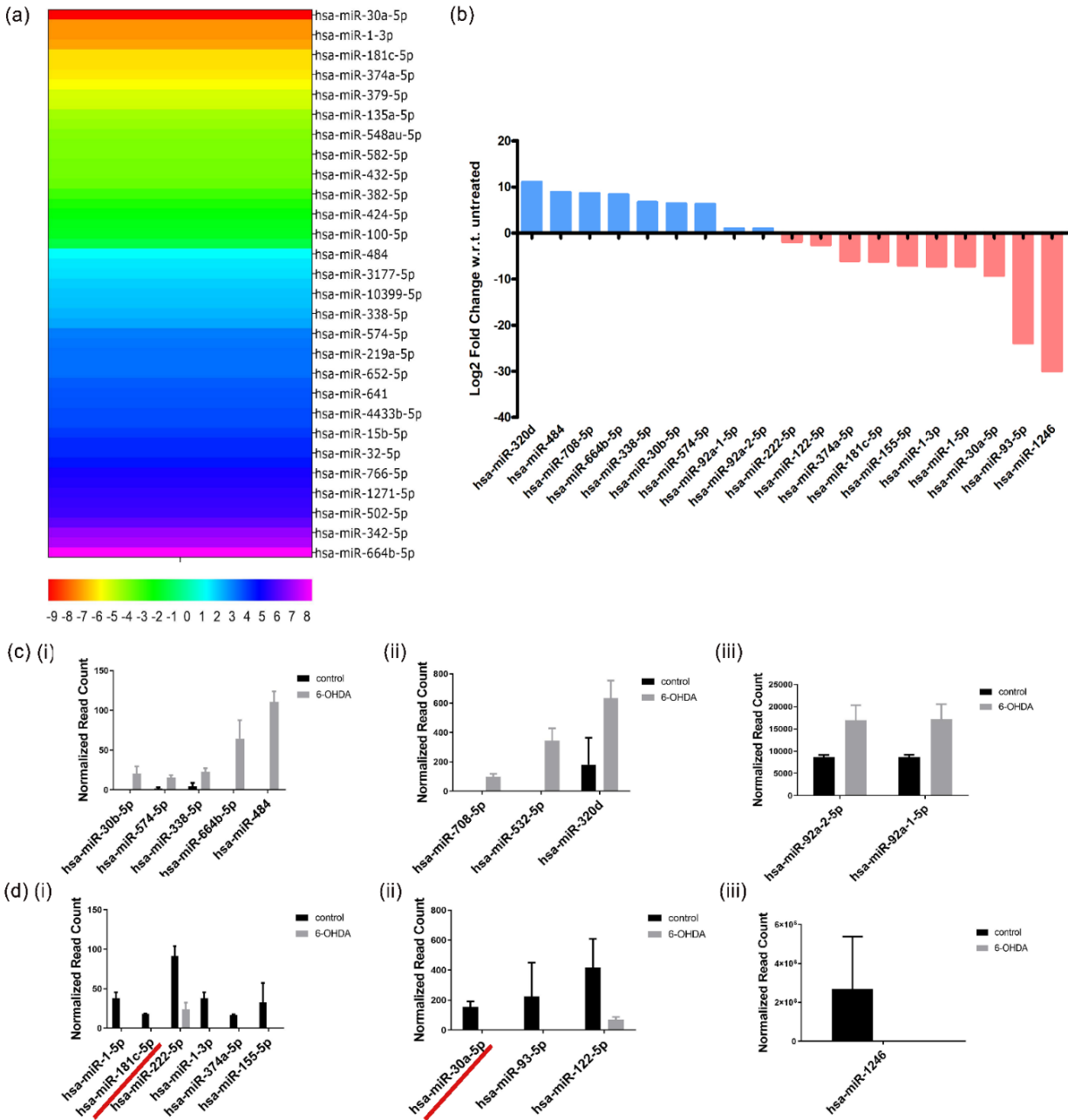


**Figure 4.2.7. 6-OHDA treatment leads to differential miRNA enrichment in SK-N-SH exosomes:** (a) Heatmap showing log2 fold change of miRNA levels (treatment/control) in exosomes from SK-N-SH neuronal cells treated with 6-OHDA. (b) Differential expression of miRNAs in exosomes under PD stress conditions analyzed from NGS data. (c, d) Upregulated miRNAs (c) and downregulated miRNAs (d) Arranged according to the read counts in exosomes: (i) <100 (ii) 100-1000 and (iii) >1000. Underline indicates that hsa-miR-181c-5p and hsa-miR-30a-5p were validated by RT-qPCR in the further part of the study and were selected for further functional analyses.

Putative target pathways were determined by selecting all miRNAs of each category, the combination of all five target prediction tools, and ClipSeq with low stringency and a corrected p value <0.05. The GO terms and pathways were retrieved for each category and tabulated (Fig 4.2.8, Fig 4.2.9). The primary subcellular compartment modulated by the targets of differentially enriched exosomal miRNAs were the nucleus and cytoplasm, although some targets also localized to the endosomal system. The targets of the identified upregulated miRNAs encode proteins localized in the mitochondrial outer membrane (Fig 4.2.8(c)).

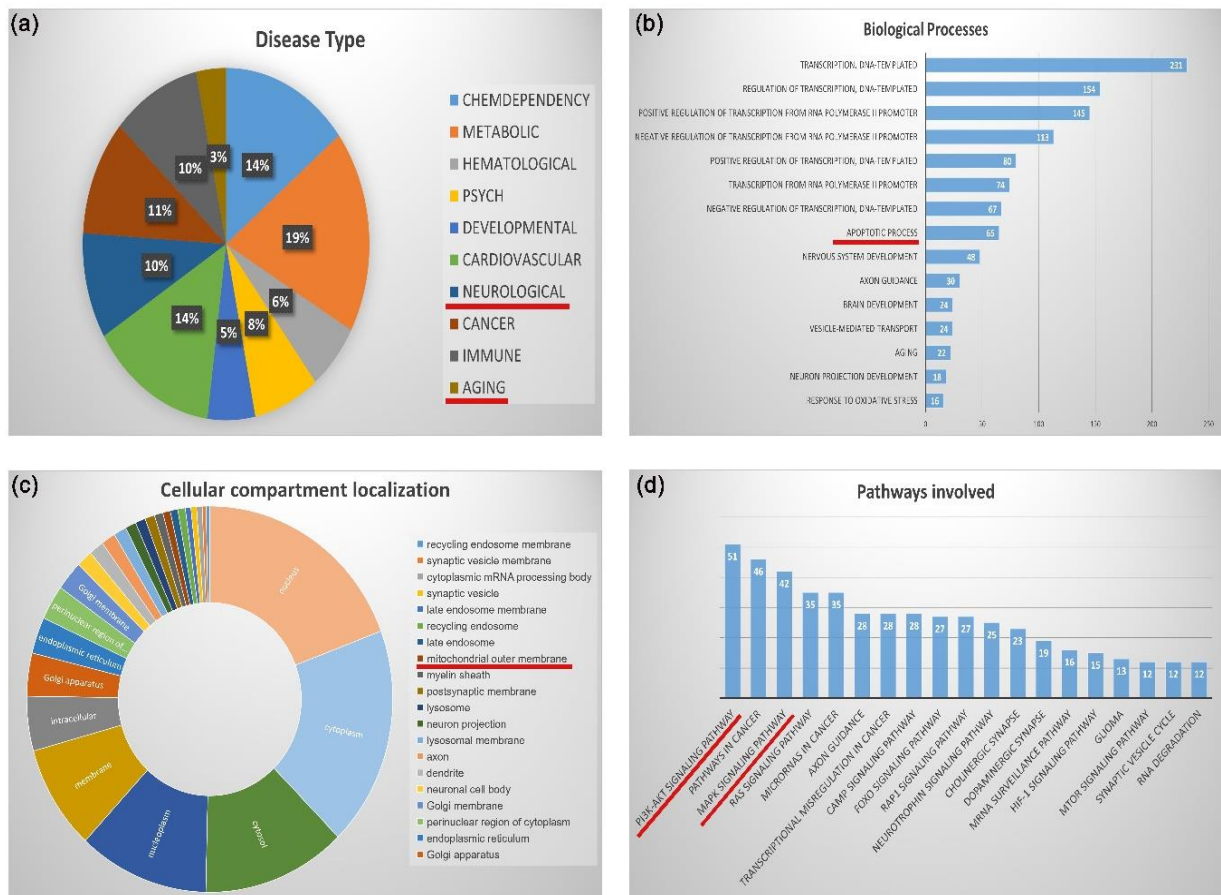


**Figure 4.2.8. Putative bioinformatic analysis of targets of upregulated exosomal miRNAs:** Target analysis of upregulated miRNAs along with their (a) diseases, (b) biological processes, (c) cellular localisation, and (d) pathways involved.

The most modulated biological process by most targets in upregulated (Fig 4.2.8(b)) and downregulated miRNAs (Fig 4.2.9(b)) is transcription. Transcription factors, like, MEF2 family, FoX family of transcription factors as well as MAPK pathway proteins can significantly alter the transcriptome of the cell when their levels are altered by the exosomal miRNAs in the recipient cell. The other critical biological processes modulated by the identified miRNAs are related to apoptosis and ageing, as well as processes related to neuronal differentiation and morphogenesis (Fig 4.2.8(b), Fig 4.2.9(b)). The major pathways involved for both classes of targets include PI3K-AKT and MAPK signalling pathways. Downregulated exosomal miRNA targets are involved in endocytosis pathways as well (Fig 4.2.9(d)). Around 10% of the upregulated targets, including FBXO8, WFDC2, ACBD5, ATXN10 (Fig 4.2.8(a)), and 13% of the downregulated targets, like, PTEN, SYN2, DNAJB1 (Fig 4.2.9(a)), are involved in neurological diseases.

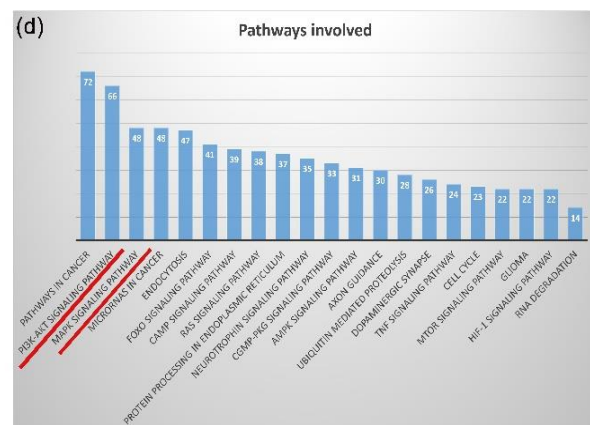
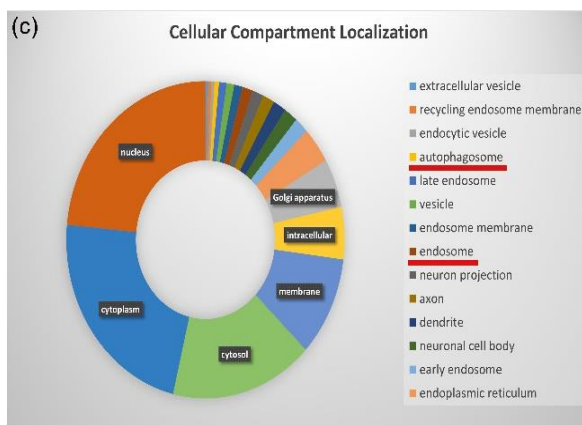
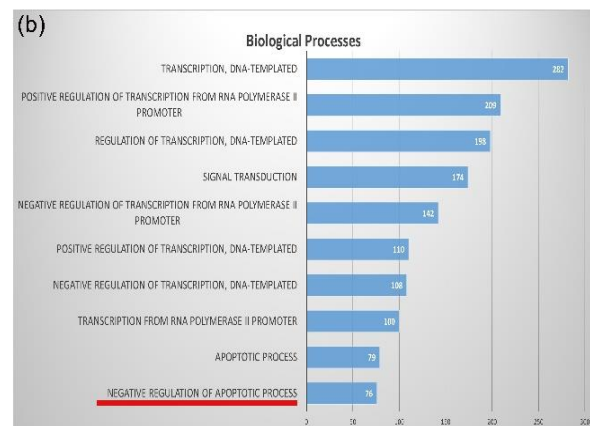
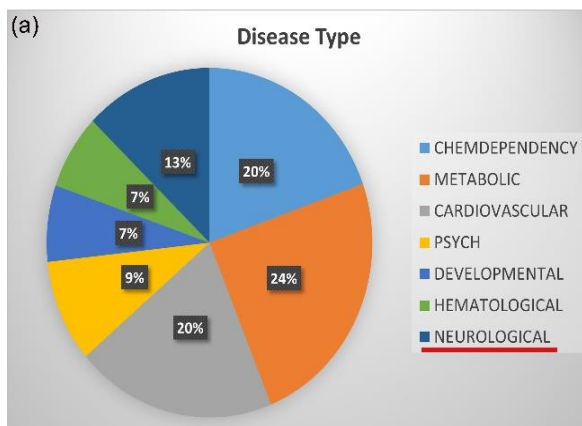


**Figure 4.2.9. Putative bioinformatic analysis of targets of downregulated exosomal miRNAs:** Target analysis of downregulated miRNAs along with their (a) diseases, (b) biological processes, (c) cellular localisation, and (d) pathways involved.

### **4.2.4 Validation of identified exosomal miRNAs in neuronal cells**

To validate the identified miRNAs that were sorted in the NGS data, the levels of selected cellular miRNAs under PD stress conditions were analyzed. SK-N-SH cells treated with 6-OHDA showed a differential expression of 7 miRNAs, and these were selected for validation by RT-qPCR. miR-664b-5p, miR-92a-1-5p, miR-181c-5p, miR-484, and miR-30a-5p were downregulated, whereas miR-320d and miR122-5p were upregulated in 6-OHDA treated SK-N-SH cells (Fig 4.2.10(a)(i)). Same miRNAs in exosomes from SK-N-SH cells in PD stress condition were also assessed. The levels of miR-181c-5p, miR-30a-5p, and miR-122-5p were significantly downregulated, which corroborated the NGS data. Additionally, miR-664b-5p showed increased levels in exosomes, in consonance with the NGS data (Fig 4.2.10(a)(ii)).

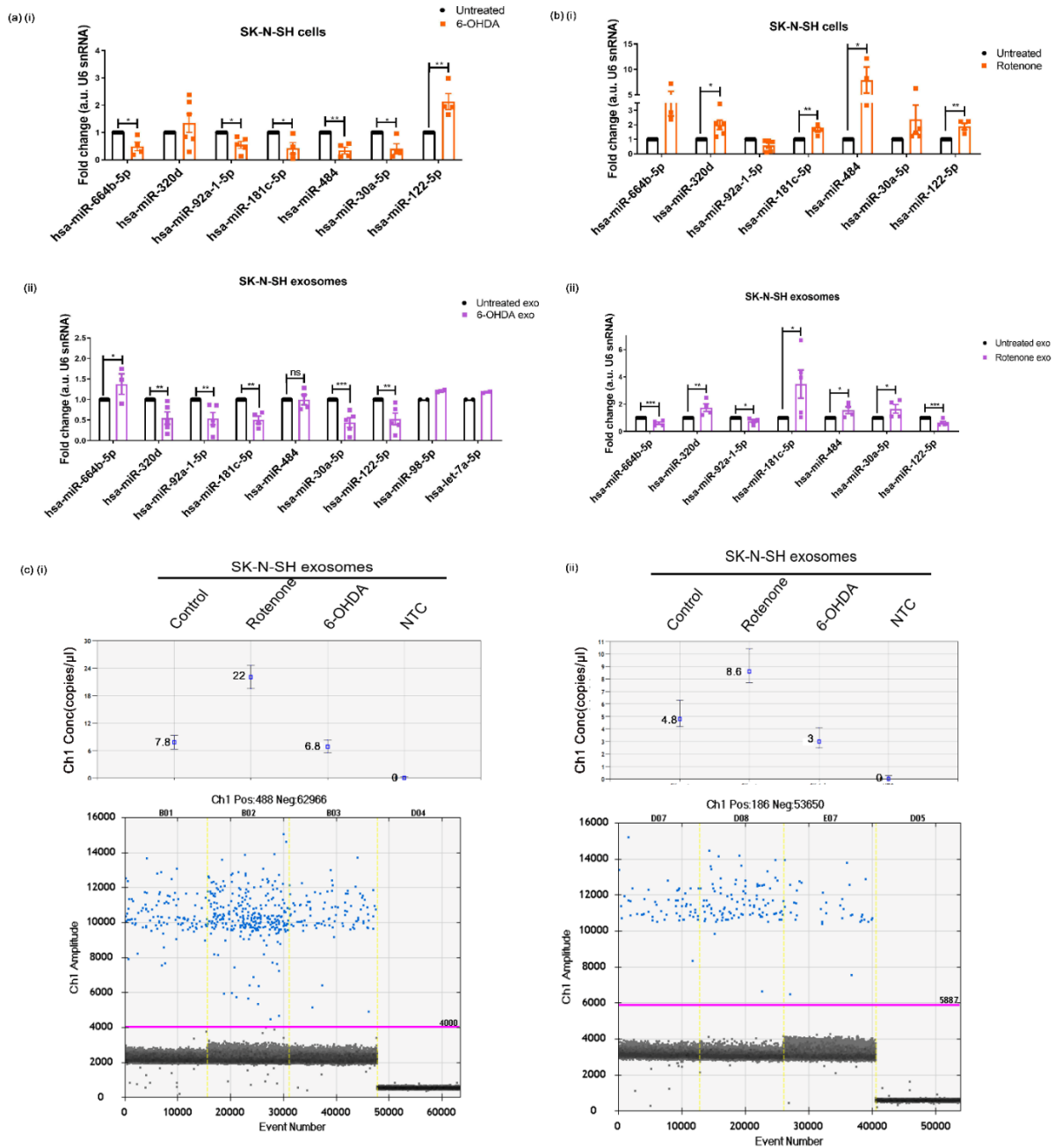


**Figure 4.2.10. Validation of miRNAs from NGS in SK-N-SH neuronal cells and exosomes:** (a) SK-N-SH neuronal cells were treated with 6-OHDA, and the differential expression of miRNAs in (i) total cell and (ii) exosomes was quantified by RT-qPCR. (b) SK-N-SH cells were treated with rotenone, and miRNA levels were checked in (i) total cell and (ii) exosomes by RT-qPCR. (c) Levels of (i) hsa-miR-181c-5p and (ii) hsa-miR-30a-5p were quantified in SK-N-SH 6-OHDA and rotenone exosomes by Droplet Digital PCR. Asterisk (\*), (\*\*), and (\*\*\*) indicates values statistically significant from control; p value <0.05, <0.01 and <0.001 (respectively), SEM of three independent experiments.

miRNA levels in SH-SY5Y cells were quantified by RT-qPCR. miR-30a-5p and miR-181c-5p were downregulated, whereas miR-664b-5p was enriched, in exosomes from cells treated with 6-OHDA (Fig 4.2.11(a)(i) and (ii)). In consonance with the NGS data obtained for SK-N-SH exosomes, and similarity between the two neuronal cell types, miRNAs which showed consistent and similar results across both cell lines: miR-30a-5p and miR-181c-5p were selected. Further, the levels of these miRNAs in both cell lines and their exosomes in the presence of rotenone was analyzed. Exosomes from rotenone-treated SK-N-SH (Fig 4.2.10(b)) and SH-SY5Y (Fig 4.2.11(b)) showed increased enrichment of miR-30a-5p and increased and decreased miR-181c-5p enrichment, respectively.

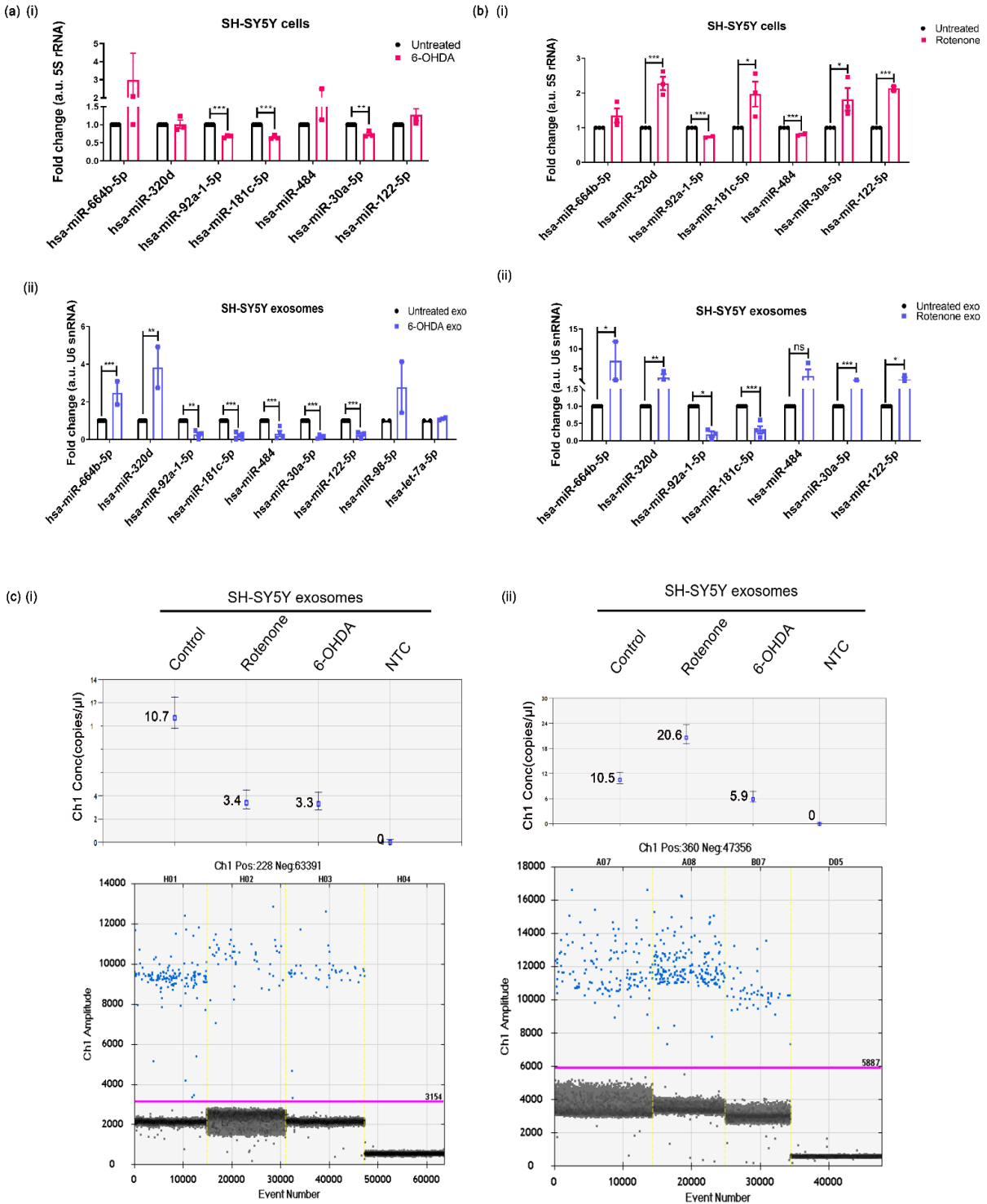


**Figure 4.2.11. Validation of miRNAs from NGS in SH-SY5Y neuronal cells and exosomes:** (a) SH-SY5Y neuronal cells were treated with 6-OHDA, and the differential expression of miRNAs in (i) total cells and (ii) exosomes was checked by RT-qPCR. (b) SH-SY5Y neuronal cells were treated with rotenone, and miRNA levels

were checked in (i) total cells and (ii) exosomes by RT-qPCR. (c) Levels of (i) hsa-miR-181c-5p and (ii) hsa-miR-30a-5p were quantified in SH-SY5Y PD-stressed exosomes by Droplet Digital PCR. Asterisk (\*), (\*\*), and (\*\*\*) indicates values statistically significant from control; p value <0.05, <0.01 and <0.001 (respectively), SEM of three independent experiments.

The two candidate miRNAs were further validated by using the absolute quantification by droplet digital PCR (ddPCR) method. The ddPCR of SK-N-SH untreated as well as rotenone and 6-OHDA exosomes indicated the same results as obtained by RT-qPCR (Fig 4.2.10(c)). Similarly, ddPCR of SH-SY5Y exosomes also showed that miR-181c-5p decreases in both rotenone and 6-OHDA exosomes (Fig 4.2.11(c)(i)), and miR-30a-5p increases in rotenone exo but decreases in 6-OHDA exo (Fig 4.2.11(c)(ii)).

Further, we validated the candidate miRNA levels in primary neuronal cultures from rat embryos. The results clearly indicate that the level of miR-30a-5p and miR-181c-5p decreases in both primary cortical and midbrain neurons when treated with rotenone (Fig 4.2.12(a)) and decreases in the rotenone exosomes from the primary neuronal cultures (Fig 4.2.12(b)). Although the cellular levels of both the miRNAs are not altered significantly when primary neurons are treated with 6-OHDA (Fig 4.2.12(c)), the 6-OHDA exosomes from both primary cortical and midbrain neurons show a clear decrease in both miR-30a-5p and miR-181c-5p levels (Fig 4.2.12(d)).

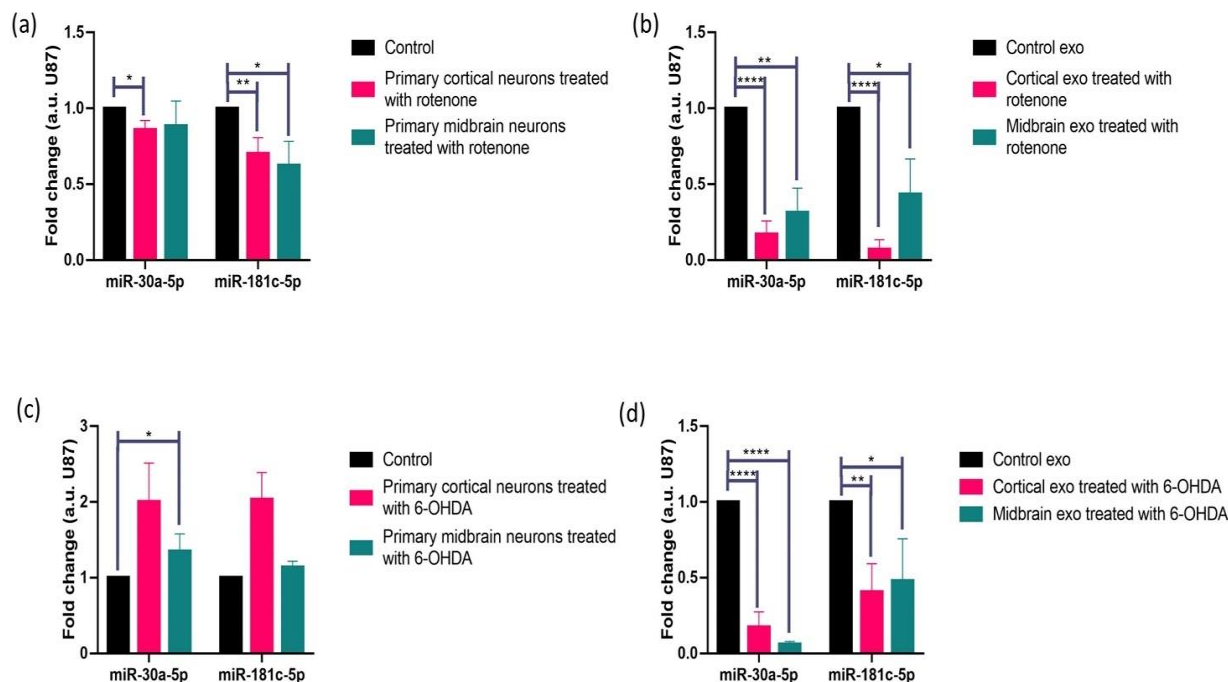


**Figure 4.2.12. Validation of miRNAs in rat primary cortical and midbrain neurons and exosomes:** Primary cortical and midbrain neurons were treated with rotenone (25nM and 60nM respectively), and the differential expression of miRNAs in (a) total cells and (b) exosomes was checked by RT-qPCR. Primary cortical and midbrain neurons were treated with 75 $\mu$ M 6-OHDA, and the differential expression of miRNAs in (c) total cells and (d) exosomes was checked by RT-qPCR. Asterisk (\*), (\*\*), (\*\*\*) and (\*\*\*\*) indicates values statistically significant from control; p value <0.05, <0.01, <0.001 and <0.0001 (respectively), SEM of three independent experiments.

#### **4.2.5 Putative target analysis of miR-30a-5p and miR-181c-5p**

Previous data indicated that miR-30a-5p and miR-181c-5p are significantly altered in exosomes in PD stress conditions. This was confirmed in two types of neuronal cell lines, SK-N-SH and SH-SY5Y, as well as in PD-stressed primary cortical and primary midbrain neurons isolated from rat embryos. Putative analysis of miR-30a-5p and miR-181c-5p revealed that both miRNAs have targets related to mitochondrial functions (Fig 4.2.13(a)), inflammation (Fig 4.2.13(b)), and cell death (Fig 4.2.13(c)), and even had some common targets, including MIGA2, SIRT1, SOCS3, PAWR, BCL2, BCLAF1 and BCL2L11.

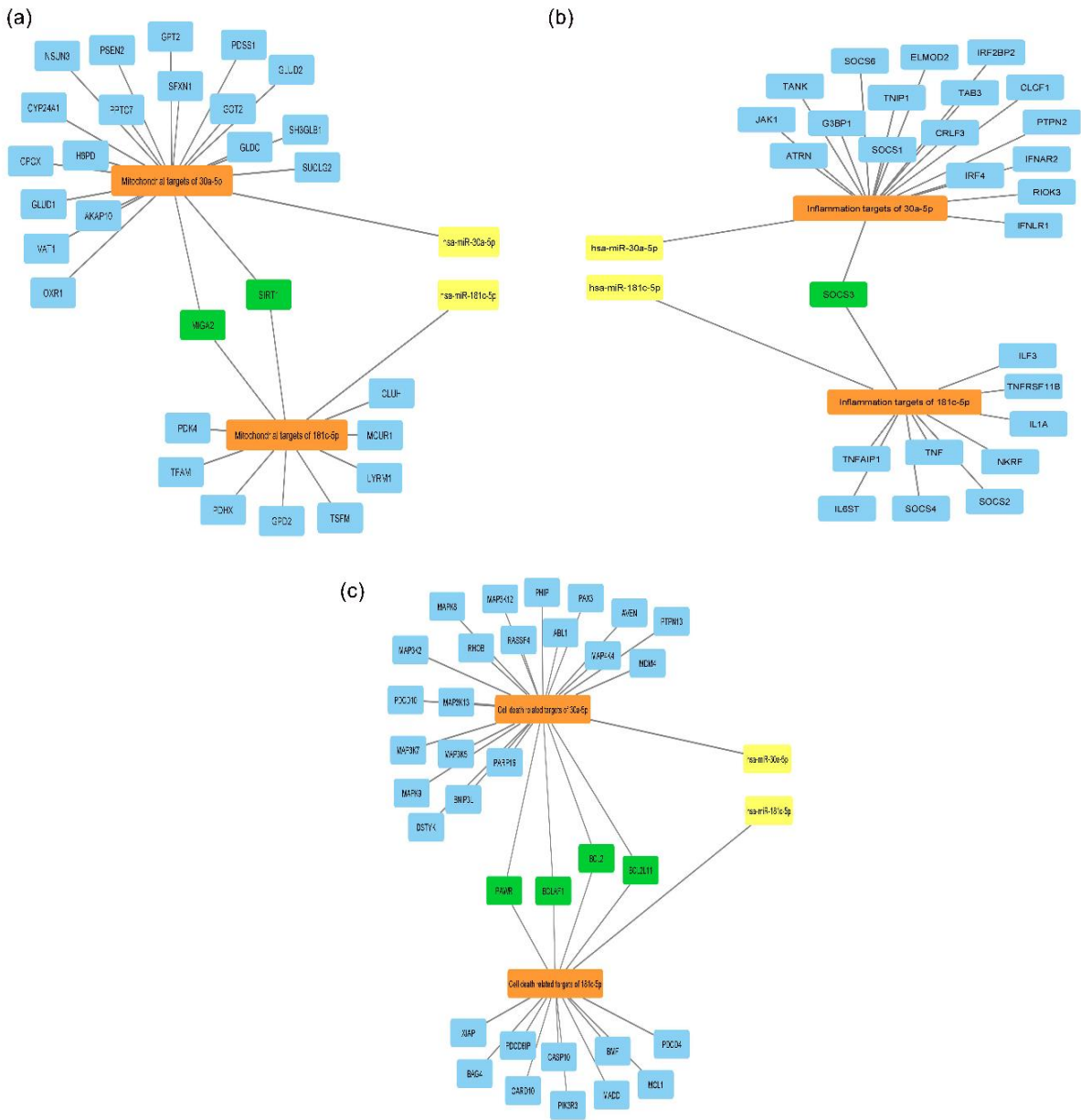
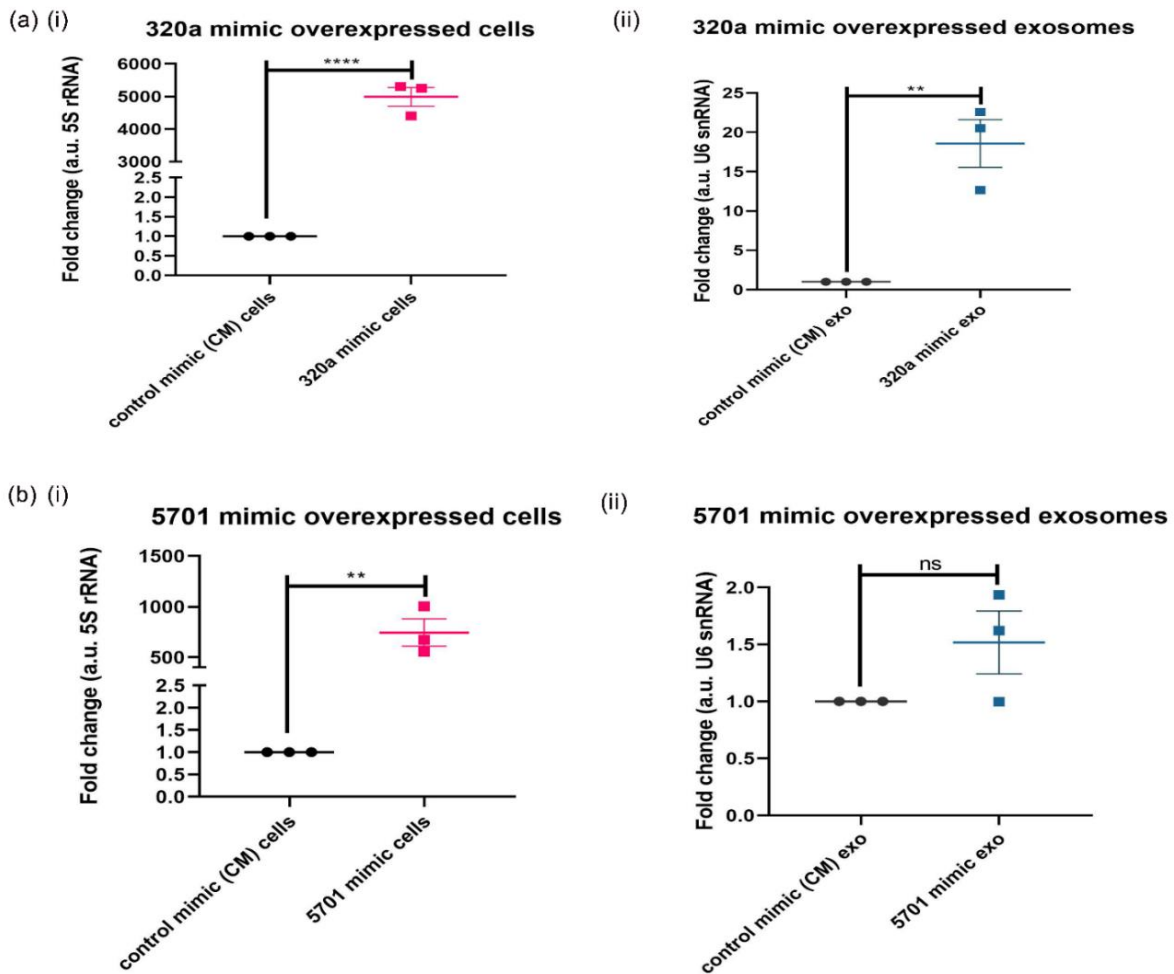


Figure 4.2.13. Cellular targets of hsa-miR-30a-5p and hsa-miR-181c-5p involved in (a) mitochondrial pathways (b) inflammation and (c) cell death.

### **4.2.6 miRNAs are selectively sorted into exosomes**

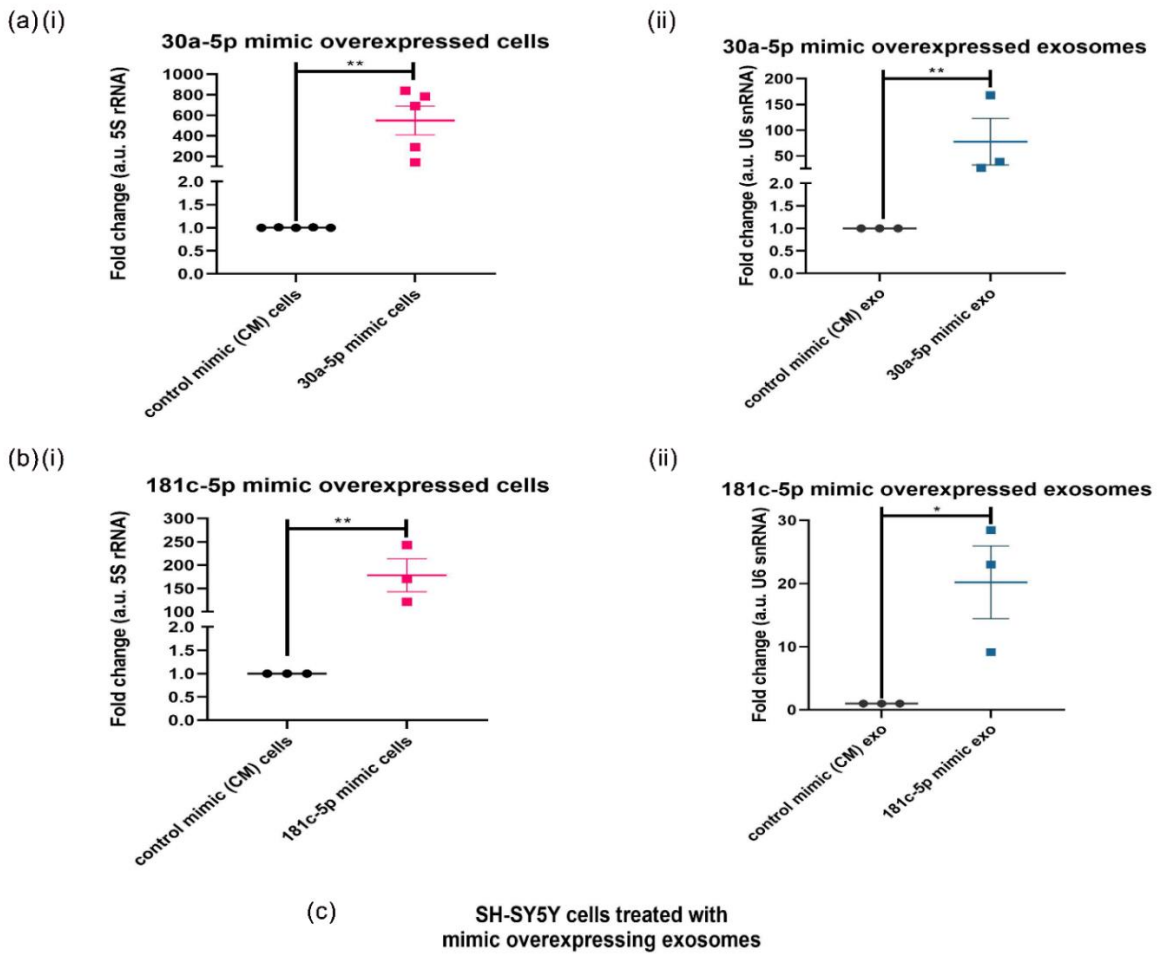
To determine whether selective enrichment of identified miRNAs in exosomes is observed in neuronal cells, mimic of miR-320a, one of the predominant exosomal miRNAs that was detected in NGS (data not shown), was transfected in SH-SY5Y cells, and subsequently exosomes were isolated, and RNA was extracted. The cells showed a significant overexpression of the miR-320a (Fig 4.2.14(a)(i)) and showed increased levels of miR-320a in exosomes as compared to control mimic (CM) exosomes (Fig 4.2.14(a)(ii)). This indicated that miR-320a is packaged into exosomes, and its enrichment in exosomes also increased upon overexpression in neuronal cells. Next, miR-5701 was selected, which was not detected in the exosomes according to the NGS data. miR-5701 mimic was transfected in SH-SY5Y cells, and RNA was isolated from the cells and released exosomes in the transfected condition. miR-5701 levels increased in the cells upon transfection of the mimic (Fig 4.2.14(b)(i)), but, unlike miR-320a, there was no accumulation of miR-5701 in exosomes (Fig 4.2.14(b)(ii)). This strongly suggests that miRNA enrichment in exosomes is specific, and even overexpression of a miRNA in cells will not lead to its selective packaging into the exosome. The results indicated that the enrichment of miRNAs to the exosomes is specific in each condition and may be cell type specific.



**Figure 4.2.14. miRNA sorting in exosomes is specific:** (a) miR-320a and (b) miR-5701 were transfected into SH-SY5Y neuronal cells. Subsequently, RNA was isolated from (i) the cells as well as (ii) their exosomes, and the levels of respective miRNAs were checked in cellular RNA and exosomal RNA by RT-qPCR. Asterisk (\*\*) and (\*\*\*\*) indicates values statistically significant from control; p value <0.01 and <0.0001 respectively), SEM of three independent experiments.

Hence, it was further determined whether the identified miRNAs (data in previous chapter), miR-30a-5p and miR-181c-5p, were enriched in exosomes when overexpressed in cells. SH-SY5Y neuronal cells were transfected with a control mimic (CM), miR-30a-5p mimic, or miR-181c-5p mimic, and subsequently exosomes were isolated from the same. Both miR-30a-5p and miR-181c-5p were highly expressed in the cells (Fig 4.2.15(a)(i), Fig 4.2.15(b)(i)) and enrichment of the miRNAs was also observed in exosomes (Fig 4.2.15(a)(ii), Fig 4.2.15(b)(ii)). Further assessment

was done whether exosomes enriched with the identified miRNAs were internalized by the recipient cells. For this, exosomes isolated from SH-SY5Y cells expressing the identified miRNAs were incubated with fresh SH-SY5Y cells. After an incubation period, the recipient cells were collected, and levels of both miRNAs were checked. RT-qPCR showed that at 6h, levels of miR-30a-5p were significantly higher in cells incubated with 30a-5p-loaded exosomes as compared to control exosomes. Similarly, miR-181c-5p was significantly higher in 181c-5p mimic exo-incubated cells as compared to control exosomes (Fig 4.2.15(c)).



(c) SH-SY5Y cells treated with mimic overexpressing exosomes

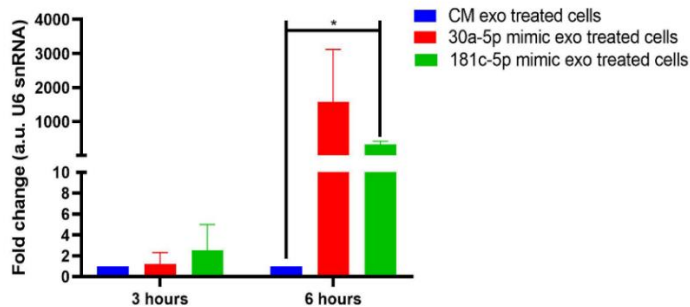


**Figure 4.2.15. miR-30a-5p and miR-181c-5p are selectively sorted in neuronal exosomes and are internalized by bystander neuronal cells:** (a) miR-30a-5p and (b) miR-181c-5p were transfected into SH-SY5Y neuronal cells. Subsequently, RNA was isolated from (i) the cells as well as (ii) their exosomes, and the levels of respective miRNAs were checked in cellular RNA and exosomal RNA by RT-qPCR. (c) SH-SY5Y neuronal cells were incubated with CM loaded exosomes, miR-30a-5p loaded exosomes, or miR-181c-5p loaded exosomes for 3h and 6h. Subsequently, RNA was isolated from the recipient cells, and the levels of both miRNAs were checked at different timepoints using RT-qPCR. Asterisk (\*), (\*\*), and (\*\*\*) indicates values statistically significant from control; p value <0.05, <0.01 and <0.001 (respectively), SEM of three independent experiments.

### **4.2.7 miR-30a-5p and miR-181c-5p mimic-loaded exosomes rescue mitochondrial dysfunction and cell death in PD-stressed neuronal cells**

Since miR-30a-5p and miR-181c-5p mimic-loaded exosomes were readily internalized by neuronal cells, further analysis of mitochondrial functions in neuronal pre-exposed to the PD stress inducers, 6-OHDA and rotenone, in the presence of miRNA-enriched exosomes was performed (Fig 4.2.16).

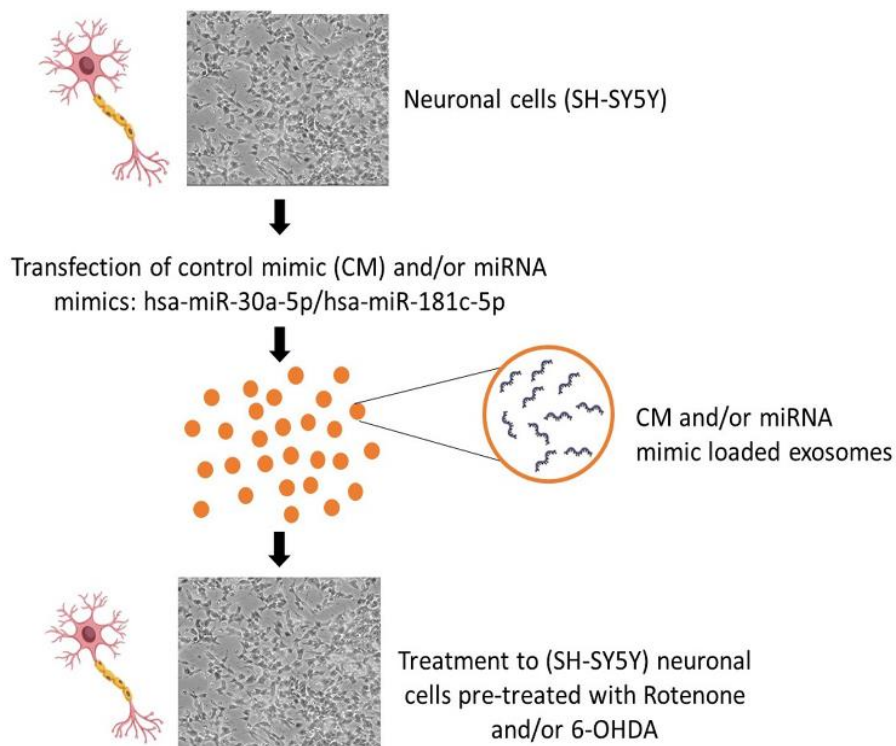


**Figure 4.2.16. Schematic flowchart showing mimic-loaded exosomes from SH-SY5Y neuroblastoma cells treated to bystander neuronal cells pre-treated with PD stress inducers.**

Total cellular ROS increased in 6-OHDA- and rotenone-treated SH-SY5Y cells (Fig 4.2.17(a)). Interestingly, following incubation with 30a-5p and 181c-5p mimic-loaded exosomes, ROS levels in the PD-stressed cells reduced as compared to control mimic (CM) exosomes (Fig 4.2.17(a)). Next, mitochondrial ROS levels were assessed in the presence of 30a-5p- or 181c-5p-loaded exosomes. Microscopic analysis indicated that 30a-5p- and 181c-5p-loaded exosomes ameliorated mitochondrial ROS levels in PD-stressed SH-SY5Y cells as compared to the control exosomes (Fig 4.2.17(b)).

Next, cell death analysis was done via the MTT assay, which indicated that miRNAs 30a-5p- and 181c-5p-loaded exosomes incubated with SH-SY5Y cells showed an increase in cell viability as compared to the CM exosomes and ameliorated cell death induced by 6-OHDA and rotenone (Fig 4.2.17(c)). Further, caspase 3/7 activity by a luminescence method in the same indicated conditions confirmed the results concordant with the cell viability assay. The caspase activity was higher in the CM-exo-incubated, PD-stressed cells and reduced when the cells were incubated with miRNA mimic-loaded exosomes (Fig 4.2.17(d)).

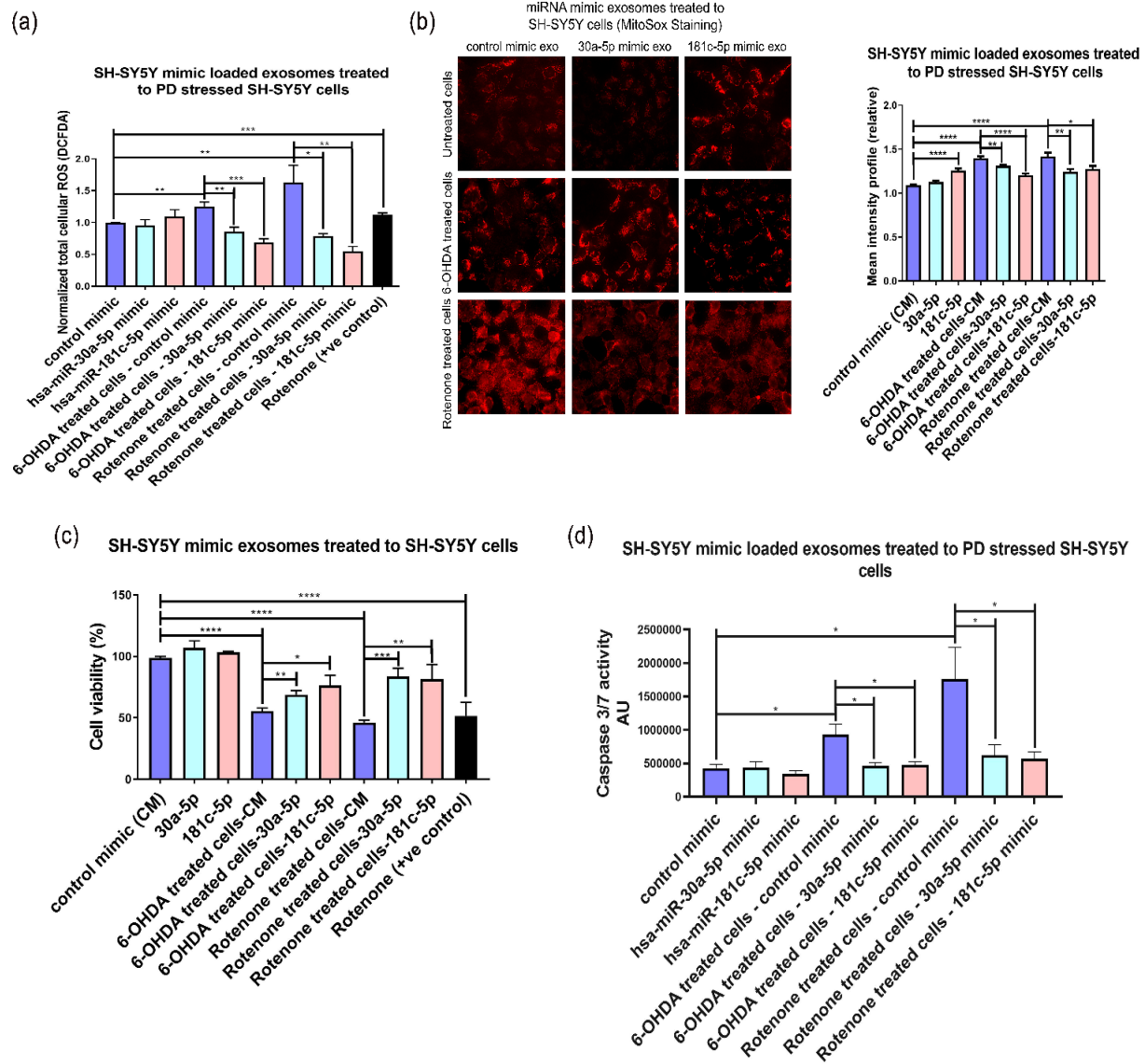


**Figure 4.2.17. miRNA mimic-loaded exosomes rescue mitochondrial dysfunction and cell death in PD-stressed neuronal cells:** (a) Mimic-loaded exosomes were incubated with SH-SY5Y neuroblastoma cells for 24h, the cells being pre-exposed to 6-OHDA or rotenone for 24h. Total cellular ROS levels were analyzed fluorometrically by H<sub>2</sub>DCFDA staining. (b) Mimic-loaded exosomes were incubated with PD-stress pre-exposed SH-SY5Y neuronal cells for 24h, and MitoSox™ levels were analyzed by fluorescence microscopy. (c) Mimic-loaded exosomes were incubated with PD-stress pre-exposed SH-SY5Y neuronal cells for 48h, and cell viability was determined by MTT assay. (d) Mimic-loaded exosomes were incubated with above-described pre-exposed SH-SY5Y neuronal cells for 48h, and caspase 3/7 levels were determined by a luminescence method. Asterisk (\*), (\*\*), (\*\*\*) and (\*\*\*\*) indicates values statistically significant from control; p value <0.05, <0.01, <0.001 and <0.0001 (respectively), SEM of two or three independent experiments.

Total cellular ROS levels by DCFDA staining in mimic exo treated U-87 MG glial cells indicated that 181c-5p mimic exosomes rescue the ROS levels which are increased due to the 6-OHDA and Rotenone treatment, and 30a-5p mimic exosomes also shows a rescue effect on 6-OHDA treated cells as compared to the CM exosomes (Fig 4.2.18(a)).

Mitochondrial ROS levels by MitoSox staining in the presence of 30a-5p and 181c-5p loaded exosomes in U-87 MG glial cells, which were pre-exposed to 6-OHDA and Rotenone, did not show a significant difference (Fig 4.2.18(b)). This indicated that in U-87 MG glial cells, the total cellular ROS levels are rescued, but no difference is observed in the mitochondrial ROS levels.

Next, cell death via MTT assay indicated that in U-87 MG cells; the miRNAs 30a-5p and 181c-5p loaded exosomes showed an increase in cell viability as compared to the CM exosomes and ameliorated the cell death that is induced by 6-OHDA and rotenone (Fig 4.2.18(c)). Further, levels of caspase 3/7 by luminescence method in the similar above indicated conditions showed results which were concordant with the cell viability assay. The caspase activity, which was higher in the CM-exo treated PD stressed cells, is reduced when the cells are treated with miRNA mimic loaded exosomes (Fig 4.2.18(d)).

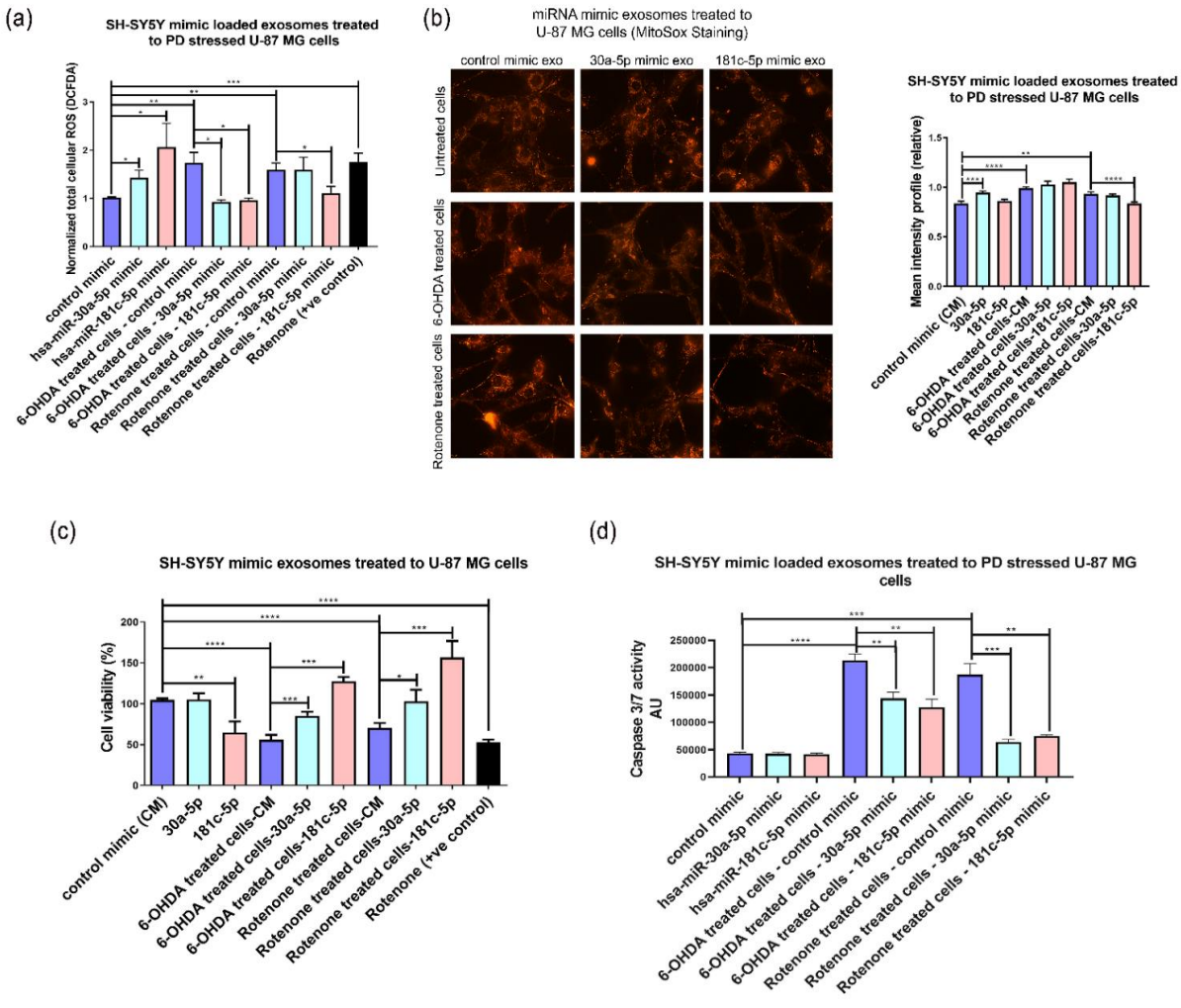


**Figure 4.2.18. miRNA mimic-loaded exosomes rescue mitochondrial dysfunction and cell death in PD-stressed glial cells:** (a) Mimic-loaded exosomes were incubated with U-87 MG glial cells for 24h, the cells being pre-exposed to 6-OHDA or rotenone for 24h. Total cellular ROS levels were analyzed fluorometrically by H<sub>2</sub>DCFDA staining. (b) Mimic-loaded exosomes were incubated with PD-stress pre-exposed U-87 MG glial cells for 24h, and MitoSox™ levels were analyzed by fluorescence microscopy. (c) Mimic-loaded exosomes were incubated with PD-stress pre-exposed U-87 MG glial cells for 48h, and cell viability was determined by MTT assay. (d) Mimic-loaded exosomes were incubated with above-described pre-exposed U-87 MG glial cells for 48h, and caspase 3/7 levels were determined by a luminescence method. Asterisk (\*), (\*\*), (\*\*\*) and (\*\*\*\*) indicates values statistically significant from control; p value <0.05, <0.01, <0.001 and <0.0001 (respectively), SEM of two or three independent experiments.

### **4.2.8 Discussion**

PD relevant pathology occurs in several brain regions, though the primary focus of most research is on dopaminergic neurons of the substantia nigra. Importantly, PD pathology eventually spreads to different brain regions, including the cortical areas, then the neocortex, finally spreading to the primary sensory areas and the primary motor field [82]. Neurons in the brain interact with other cells, including microglia, astrocytes, and oligodendrocytes, in terms of sharing metabolic support and coordinating responses to pathogenic stimulation. This communication also promotes the progression of neurodegeneration by propagating harmful molecules and/or toxic protein aggregates [305] via intercellular communication. Exosomes are one of the major biological carriers modulating intercellular communication in various neurological disorders. Previous data and other reports have shown that exosome release is enhanced during PD stress conditions due to interorganellar crosstalk [306], [307]. However, the fate of the released exosomes in these pathological conditions is still not understood. The current study aimed to investigate in detail the uptake of exosomes, their internalization and colocalization with mitochondria, and their alteration of mitochondrial functions and the miRNA cargo that is altered due to PD stress conditions in neuronal cells.

The data proved that exosomes originating from glial cells and neuronal cells are readily internalized by healthy bystander neuronal cells. Exosomes released from stimulated cortical neurons are preferentially taken up by neurons at their synapses, as compared to the exosomes derived from neuroblastoma cells which are internalized by both neurons and glial cells [308]. Exosome uptake has been reported to occur through endocytosis in PC12 cells, and the exosomes, after internalization, enter the endocytic pathway and are targeted to the lysosomes [309], [310]. However, the interaction of exosomes with other organelles in neurons and other cell types in the brain is not well understood. In the current study, it was observed that internalized exosomes localize to mitochondria. The uptake of exosomes isolated from neurons under PD stress conditions further led to the alteration of mitochondrial functions which was evident by alterations in mitochondrial membrane potential and ROS levels in SH-SY5Y neuroblastoma and U-87 MG glial cells, resulting in a decrease in cellular viability. Hence, exosomal cargo from PD-stressed cells brings about functional implications when internalized by bystander cells.

Exosomes have an active cargo content which can modulate various physiological functions and signalling pathways in recipient cells [311]. Intercellular RNA transfer of the gene *Arc* occurs through extracellular vesicles across the synaptic clefts of neurons, which in turn facilitates intercellular signalling to control synaptic function and plasticity [312]. The current study specifically focused on exosomal miRNAs; however, the transfer of exosomal mRNA is a possibility and may have important implications and needs to be further investigated. Previous reports have demonstrated that small RNA including miRNAs [313]–[316] can translocate to mitochondria. However, the mechanisms remain elusive. Emerging studies suggest that nuclear-encoded miRNAs translocate to mitochondria have a role in modulating mitochondrial functions and enhancing the progression of PD [317]–[319].

Many miRNAs have been shown to be involved in the pathogenesis of PD, but their packaging into exosomes, transfer to bystander cells, and modulation of mitochondrial functions is yet elusive. Hence, exosomal miRNAs and their potential implication in mitochondrial functions in neuronal cells is investigated. NGS analysis indicated that a few miRNAs are differentially sorted into exosomes under PD stress conditions. Bioinformatics analysis of the targets of the differentially expressed miRNAs showed that the major cellular compartment localization lies in the nucleus, with some targets also localized in the endosomal system. Interestingly, targets of some of the identified miRNAs consist of proteins localized in the outer mitochondrial membrane. Several reports suggest that the outer membrane of mitochondria may provide a platform for miRNA/mRNA interactions, which may determine the threshold of nuclear-encoded mRNA translation to regulate the protein level in mitochondria [320], [321]. Interestingly, the transport of mRNA to mitochondria is more evident in neurons, which have defined sub-neuronal compartments like axons, dendrites, etc., since the dynamic localization of the organelle differs within neuronal sub-compartments [322]. The cellular compartmentalization of the upregulated miRNAs in the NGS data localizes to the mitochondrial outer membrane, and these proteins may facilitate the miRNA/mRNA interactions for regulation protein levels and the mitochondrial functions. Hence, the localization of exosome-derived miRNAs in recipient neuronal cells to mitochondria is an interesting finding and should be investigated further for functional implications in intercellular and intracellular communication.

Overall, the NGS analysis indicated few miRNAs that were altered in SK-N-SH exosomes under PD stress conditions. Corroborating the results of NGS, the miRNAs hsa-miR-30a-5p and hsa-miR-181c-5p showed downregulation in exosomes in SK-N-SH as well as SH-SY5Y neuronal cells under 6-OHDA conditions. SH-SY5Y is a thrice-subcloned cell line that is derived from SK-N-SH cells. But due to various reasons, SH-SY5Y cells stands out for being widely used in neuroscience research, including its expression of several neural markers and synthesis of neurotransmitters, and they differentiate into a more human neural phenotype [323], [324]. Using this rationale, the exosomal miRNAs were validated in SH-SY5Y cell lines along with the SK-N-SH cell line, and further used only those miRNAs which showed a consistent result across both cell types. Moreover, 6-OHDA- and rotenone-exo derived from primary cortical and midbrain neurons from rat embryos also show a reduced level of both miRNAs, miR-30a-5p and miR-181c-5p. Although, miR-30a-5p is upregulated in rotenone-exo in SH-SY5Y and both miRNAs are upregulated in rotenone-exo derived from SK-N-SH cells. This indicates that the upregulation or downregulation of exosomal miRNAs are different depending on the cell lines and primary culture.

This study demonstrates that exosomes are mediators of intercellular communication between neurons during PD stress conditions. Exosomes are actively internalized by recipient neuronal cells and further localize to mitochondria. Profiling of exosomal miRNAs from neuronal cells exposed to 6-OHDA showed that selected miRNAs are differentially sorted into exosomes under PD stress conditions.

The packaging of miRNAs into exosomes is specific, as per the observation that miRNA-320a, which in consonance with NGS data, showed selective sorting in exosomes upon its expression in neuronal cells, whereas miR-5701 showed no enrichment. Further, specific enrichment of the selected miRNAs miR-30a-5p and miR-181c-5p into exosomes was observed using RT-qPCR upon expression of their corresponding mimics. Reports show that miRNA packaging into exosomes can be sequence motif-dependent, or based on modifications of RNA-binding proteins, or even dependent on raft-like regions of membranes that select for the incorporation of miRNAs into the vesicle [233], [236], [325], [326]. However, the specific presence of a sequence motif or RNA-binding protein-mediated enrichment in exosomes needs to be further investigated.

Both the miRNAs have putative targets involved in the cell death pathway, inflammation related genes, as well as mitochondrial targets. Since mitochondria is the central hub for the cell's ATP

synthesis and maintenance of cellular homeostasis, the alteration of the targets that localize with this organelle will alter the functions hereby bringing about an overall change in the cell's physiological status. Several targets of miR-30a-5p and miR-181c-5p localize to mitochondria, consistent with previous reports [327], [328].

miR-30a-5p- and miR-181c-5p-loaded exosomes ameliorated the ROS levels that were induced in the presence of PD stress conditions in SH-SY5Y neuroblastoma and U-87 MG glial cells. Surprisingly, when mitochondrial ROS levels were checked, the neuronal cells showed a rescue effect, but not the glial cells. The rescue that was observed in glial cells by both miRNA-loaded exosomes, was not dependent on the mitochondrial ROS levels, but rather the cellular ROS levels. A previous report suggested that miR-181c-5p is localized to mitochondria [329], further suggesting that exosome uptake and colocalization with mitochondria may play an important role in the physiological status of the cell.

Similarly, miR-181c-5p is known to regulate mitochondrial genome expression via targeting mt-COX1, ultimately causing electron transport chain complex IV remodelling [327], [329]. miR-30a-5p is known to dampen glycolysis in breast cancer by specifically targeting LDHA, hereby acting as a tumour suppressor [328]. This change in bioenergetics may be especially of significance in PD, since reports suggest that a slow loss of complex-I function by Ndufs2 deletion causes metabolic reprogramming in dopaminergic neurons, switching from OXPHOS to complete reliability on glycolysis [330]. In a previous report, increased levels of TNF- $\alpha$  induced miRNA alterations in SH-SY5Y cells, leading to changes in complex-I [331]. Therefore, it will be interesting to further investigate if miR-30a-5p and miR-181c-5p regulates mitochondrial complex-I/IV by modulating the specific subunits of these complexes. Further, a recent report suggests that miR-30a-5p inhibits the inflammatory pathways in microglia and astrocytes and rescues LPS-induced apoptosis [332]. miR-181c-5p has also been detected circulating in plasma and serves as a biomarker in Alzheimer's disease [333]. miR-181c-5p also inhibits the expression of proinflammatory cytokines and apoptosis to assuage spinal cord injury [334]. These observations suggest that mitochondrial function and mitochondria-mediated inflammation are modulated by miR-30a-5p and miR-181c-5p, a concept that needs to be further investigated. Although both miR-30a-5p and miR-181c-5p show a rescue with respect to mitochondrial

functions, it should be kept in mind that in physiological conditions, many miRNAs work together in a combinatorial manner to overall affect the cellular functions, and not just one or two.

Furthermore, both miR-30a-5p- and miR-181c-5p-loaded exosomes were able to rescue cell death in SH-SY5Y cells as well as U-87 MG glial cells under PD stress conditions. Both miR-181c-5p and miR-30a-5p share some common targets, including BCL2L1 apoptotic activator protein, and the pro-apoptotic WT1 regulator (PAWR), which we validated in SH-SY5Y neuronal cells (data not shown here). Exosomal miR-30a-5p and miR-181c-5p may regulate apoptotic pathways in the recipient cells, hence showing rescue under PD stress conditions. The exact targets of miR-30a-5p and miR-181c-5p in the recipient cells involved in rescuing mitochondrial functions and cell death under PD stress conditions need to be further investigated using RNA-IP experiments, and by examining the subcellular localization of the target mRNAs and proteins in neurons. The above results strongly suggest that miR-30a-5p and miR-181c-5p levels are decreased in neuronal exosomes under PD stress conditions, and that exosome-mediated transfer of miRNAs can alleviate cell death under PD stress conditions. The study suggests that exosome-mediated transfer of miRNAs plays an important role in the progression of PD, and that delivery of miR-30a-5p and miR-181c-5p through exosomes may yield novel strategies to combat the spread of PD.

**4.3 - Rotenone induced exosomal  
miRNA alterations in rat  
cerebrospinal fluid and serum induces  
mitochondrial dysfunction and cell  
death**

### 4.3.1 Rotenone toxicity in primary neurons of rat embryos affects the exosome release

Exosome release varies in different patho-physiological conditions, including different acute and chronic neuronal insults, however this has not been systemically investigated yet. Hence, the influence of rotenone toxicity in primary neurons from rat embryos on the exosome release was analyzed. Primary midbrain and cortical neurons were first treated with different rotenone doses for 24h (acute exposure) to determine the dose-dependent response and the lethal dose. Cell death assay by MTT indicated that significant cell death was observed at 25nM in primary midbrain neurons whereas the primary cortical neurons required 60nM (Fig 4.3.1(i)(a) and (ii)(a)). The lethal dose was also confirmed by the DNA damage ELISA of different rotenone concentrations which showed similar results (Fig 4.3.1(i)(b) and (ii)(b)).

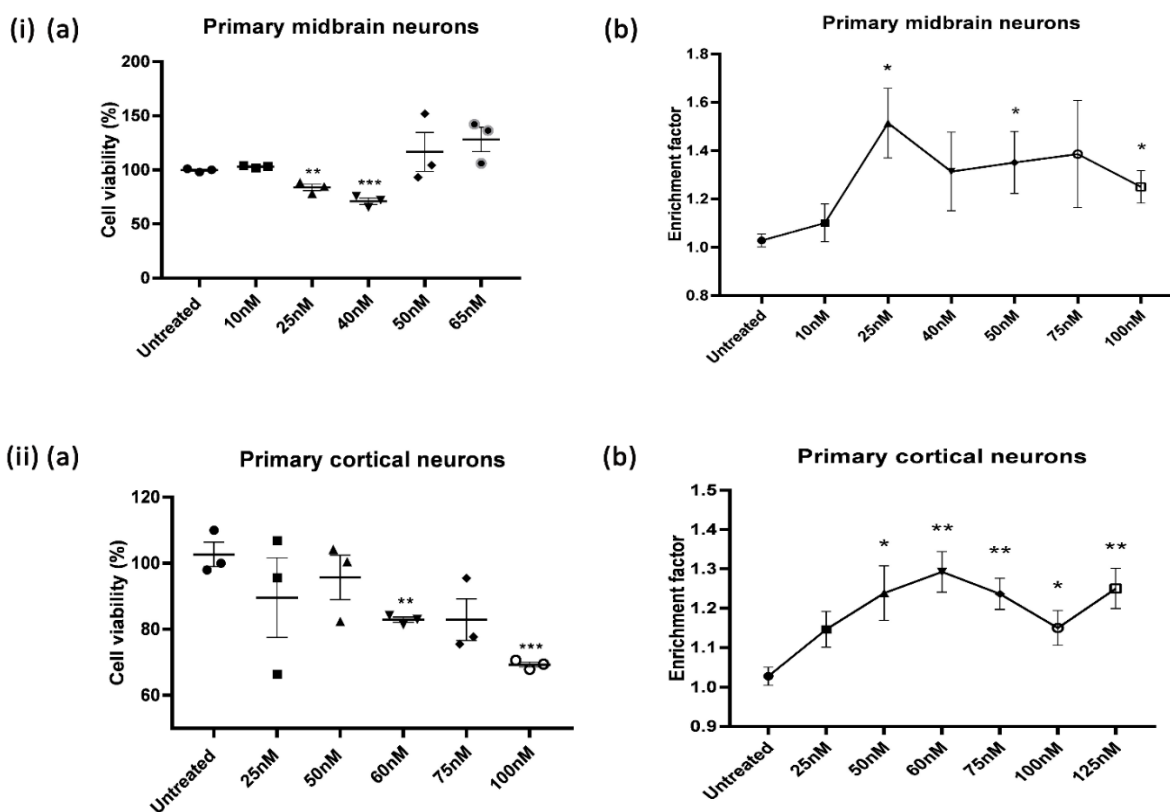


**Figure 4.3.1. Dose-dependent toxicity of rotenone in primary neurons:** (i) Primary midbrain neurons and (ii) primary cortical neurons were treated with different doses of rotenone as mentioned above for 24h and cell viability was assessed by (a) MTT cell viability assay at 570nm and (b) cell death detection by ELISA at 405nm. Asterisk (\*), (\*\*), and (\*\*\*) indicates values statistically significant from control; p value <0.05, <0.01 and <0.001 (respectively), SEM of three independent experiments, data was analyzed using Student's t-test.

Hence, for further experiments, dose 25nM for midbrain neurons and 60nM for cortical neurons was used. Primary neurons were treated with rotenone and the concentration of exosomes released was assessed by NTA. Both primary midbrain neurons as well as primary cortical neurons treated with rotenone showed enhanced exosome release and concentration increases (Fig 4.3.2(i) and (ii)).

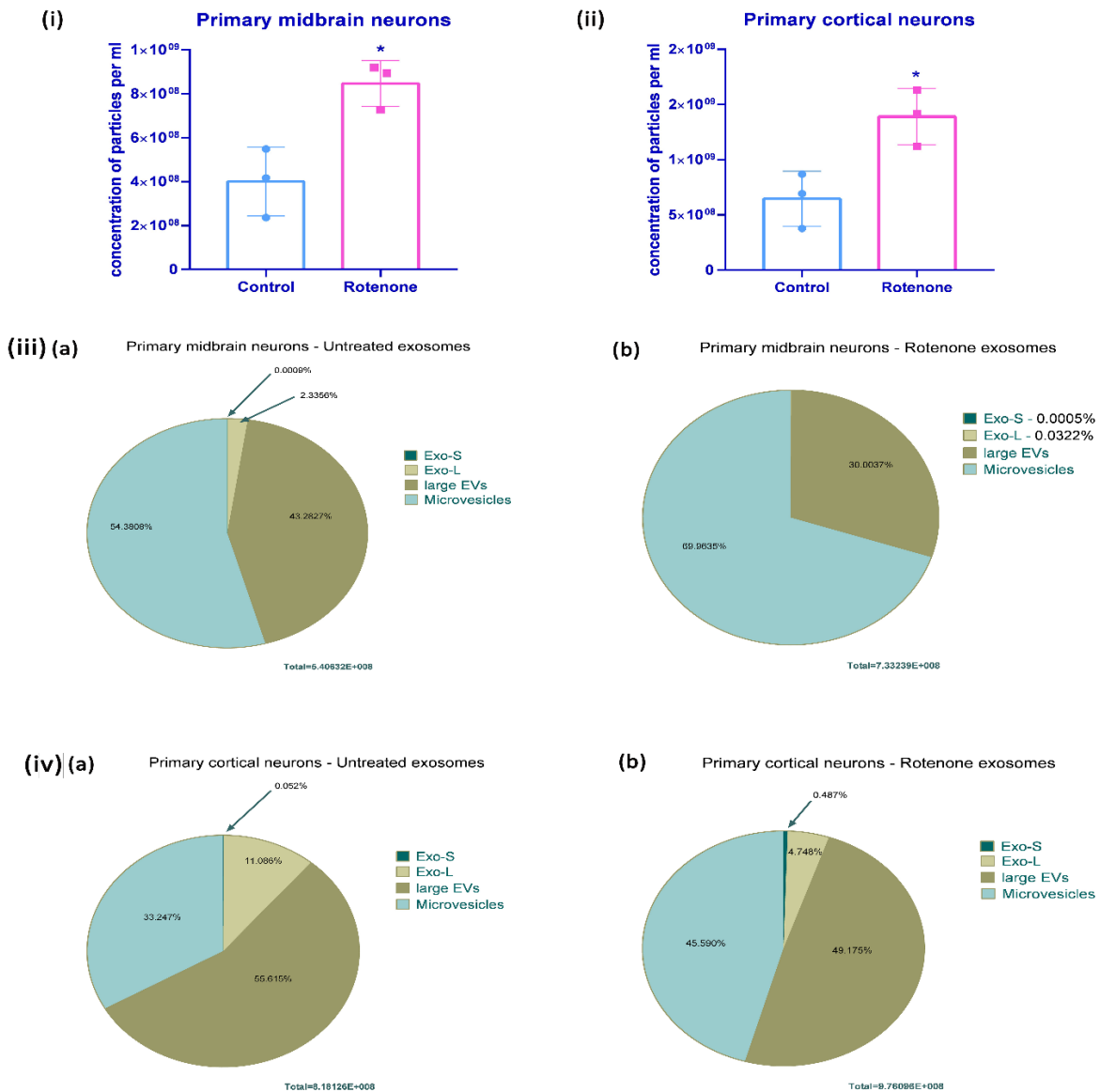


**Figure 4.3.2. Exosome release is enhanced in primary neurons on treatment of the PD-stress inducer rotenone:** (i) Primary midbrain neurons and (ii) primary cortical neurons were treated with 25nm and 60nm of rotenone, respectively, for 24h and the media was collected post-treatment and subsequently exosomes were isolated. The exosome concentration of the samples were determined using Nanoparticle Tracking Analysis (NTA), which depicts

the concentration of particles per ml of solution. Asterisk (\*) indicates value statistically significant from control; p value <0.05, SEM of three independent experiments, data was analyzed using Student's t-test. (iii) Percentage distribution of population of extracellular vesicles (EVs) derived from (a) untreated primary midbrain neurons, (b) rotenone treated primary midbrain neurons, (iv) (a) untreated primary cortical neurons and (iv) (b) rotenone treated primary cortical neurons.

Exosomes are known to be heterogenous in nature, and different subpopulations of exosomes are responsible for different biological functions. The subpopulation of exosomes was plotted based on the size difference into four kinds of groups: exomeres (~35nm), Exo-S (60-80nm), Exo-L (90-150nm), large EVs (150-500nm) and microvesicles (500-1500nm). Exomere population in the primary neuron exosomes in untreated as well as in rotenone conditions were not detected. The major subpopulation in primary midbrain neurons was microvesicles, while large EVs was the dominant subpopulation in primary cortical neurons (Fig 4.3.2(iii) and (iv)). The populations Exo-L and large EVs was lower in rotenone conditions as compared to untreated in both of primary neurons, however microvesicles subpopulation increased (Fig 4.3.2(iii) and (iv)).

### **4.3.2 Exosome release is altered in acute rotenone-treated rat models**

Further, acute rotenone toxicity induced exosome release observed *in vitro* was analyzed *in vivo*. For this, acute rotenone model of rats, treated with 3mg/kg/day for 8h and 24h were utilized. The body weights of the rats declined markedly or significantly after treatment with rotenone for 24h, however no difference was observed after 8h of rotenone treatment (Fig 4.3.3), consistent with prior reports [335].

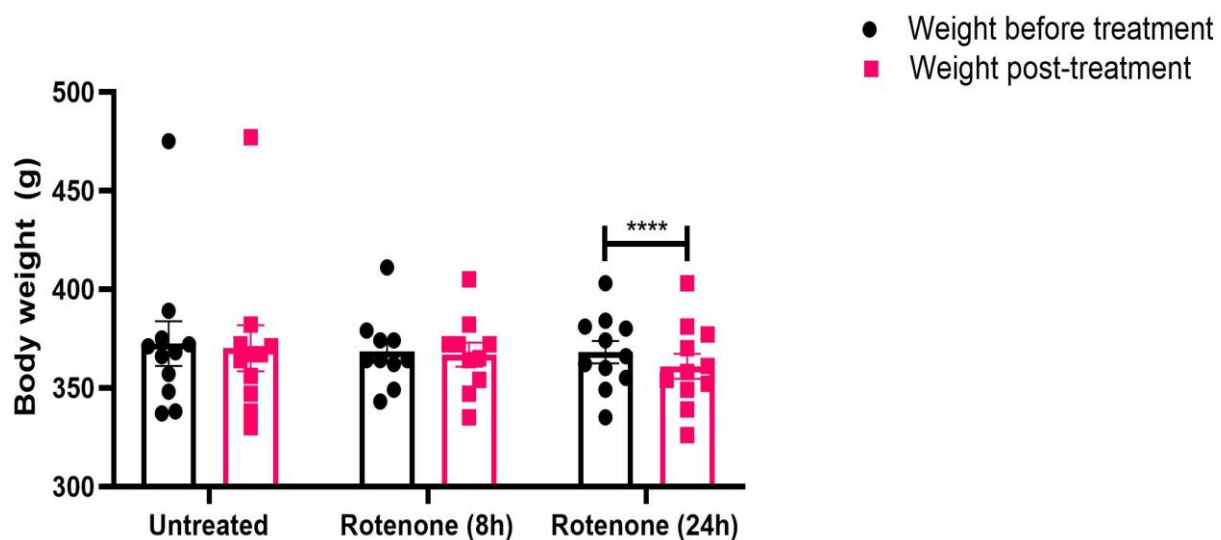


**Figure 4.3.3.** Body weights of 3-month-old male Sprague-Dawley rats recorded before and after the administration of rotenone (3mg/kg) for 8h and 24h. Asterisk (\*\*\*\*) indicates values statistically significant from control; p value <0.0001, SEM of ten independent experiments, data was analyzed using two-way ANOVA, followed by Sidak's multiple comparisons test.

Next, quantification of exosomes in the serum and cerebrospinal fluid of the rats treated with rotenone at both time points was performed. NTA analysis indicated an increase in the concentration of exosomes obtained from CSF of rotenone-treated rats however it was not significant (Fig 4.3.4(i)). The concentration of serum exosomes from rotenone-treated rats was significantly higher as compared to that of untreated rats (Fig 4.3.4(ii)).

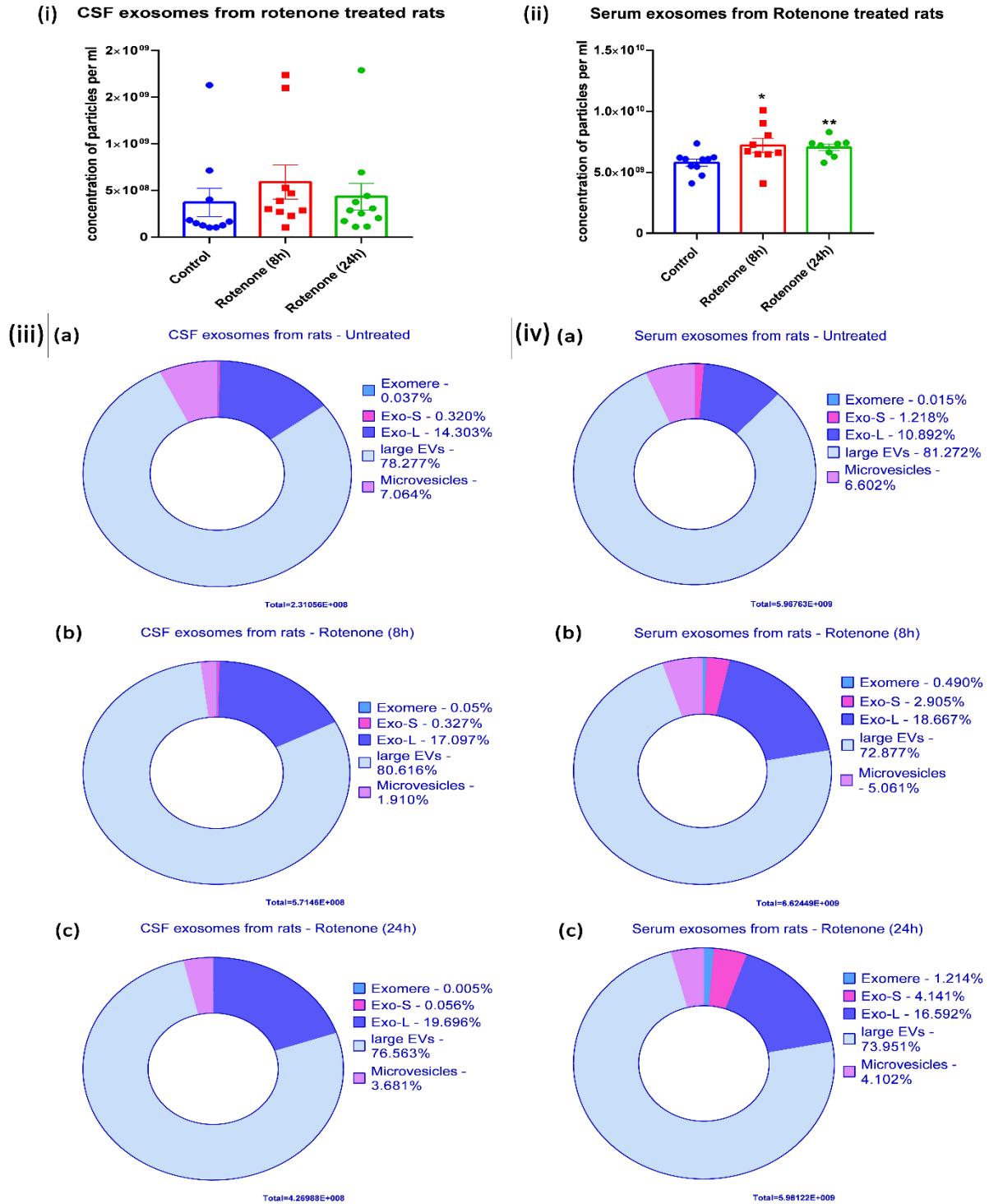


**Figure 4.3.4. Exosome release is enhanced in biofluids of acute rotenone-treated rat models of PD:** Rotenone was administered at an acute concentration of 3mg/kg to Sprague Dawley male rats of 3-months of age for 8h and 24h and subsequently exosomes were isolated from the (i) cerebrospinal fluid (CSF) and (ii) serum of healthy controls as well as treated rats post-euthanasia. The exosome concentration of the samples were determined using Nanoparticle

Tracking Analysis (NTA), which depicts the concentration of particles per ml of solution. Asterisk (\*) and (\*\*) indicates values statistically significant from control; p value <0.05 and <0.01 (respectively), SEM of ten independent values, data was analyzed using Student's t-test. (iii) Percentage distribution of population of extracellular vesicles (EVs) derived from cerebrospinal fluid (CSF) of (a) (i) untreated rats, and rats treated with rotenone (3mg/kg) for (b) 8h and (c) 24h, and (iv) serum of (a) untreated rats, and rats treated with rotenone (3mg/kg) for (b) 8h and (c) 24h.

Further, the subpopulation analysis of the CSF exosomes showed that the dominant subpopulation is large EVs. Exo-L subpopulation is higher in rotenone treated rats; however, the concentration of microvesicles decreased in the rotenone treated rats as compared to untreated (Fig 4.3.4(iii)(b) and (iv)(b)). Similarly in CSF exosomes, large EVs is the dominant subpopulation in serum exosomes as well. Surprisingly, all the three subpopulations, exomeres, Exo-S, and Exo-L, increased in serum of rotenone treated rats as compared to untreated (Fig 4.3.4(iv)). Large EVs is significantly lower in rotenone treated rats as compared to untreated, while there is no difference in the microvesicle population.

### **4.3.3 Specific miRNA levels are altered in both primary neurons and exosomes in PD stress conditions**

Exosomal specific miRNA levels specific to acute rotenone treatment in primary cortical and primary midbrain neurons was analyzed. The previous study had identified specific miRNAs which are altered under PD stress conditions in neuronal cell lines through NGS. Some of these specific miRNAs were validated in rotenone conditions in SK-N-SH and SH-SY5Y cells, which served as a rationale for the selection of the mentioned specific miRNAs for validation in the primary neurons and *in vivo* system in this study. Primary neuronal cells treated with rotenone showed altered level of miRNAs. The levels of miR-181c-5p and miR-484 were specifically significantly downregulated in the primary midbrain neurons upon rotenone treatment (Fig 4.3.5(i)(a)). The regulation pattern in cortical neurons was broader, where several miRNAs are downregulated in the primary cortical neurons on rotenone exposure, including miR-30a-5p, miR-181c-5p, miR-484 and miR-93-5p (Fig 4.3.5(ii)(a)). The levels of miR-30a-5p, miR-320a-3p, miR-484, and miR-93-5p decreased in exosomes derived from primary midbrain neurons treated with rotenone (Fig 4.3.5(i)(b)). However, the level of miR-484 increased in exosomes from primary

cortical neurons. The level of miR-30a-5p and miR-93-5p decreased in exosomes from midbrain neurons due to rotenone treatment (Fig 4.3.5(ii)(b)). The above results clearly indicated that specific miRNAs are significantly altered in exosomes and cells in response to acute rotenone toxicity.

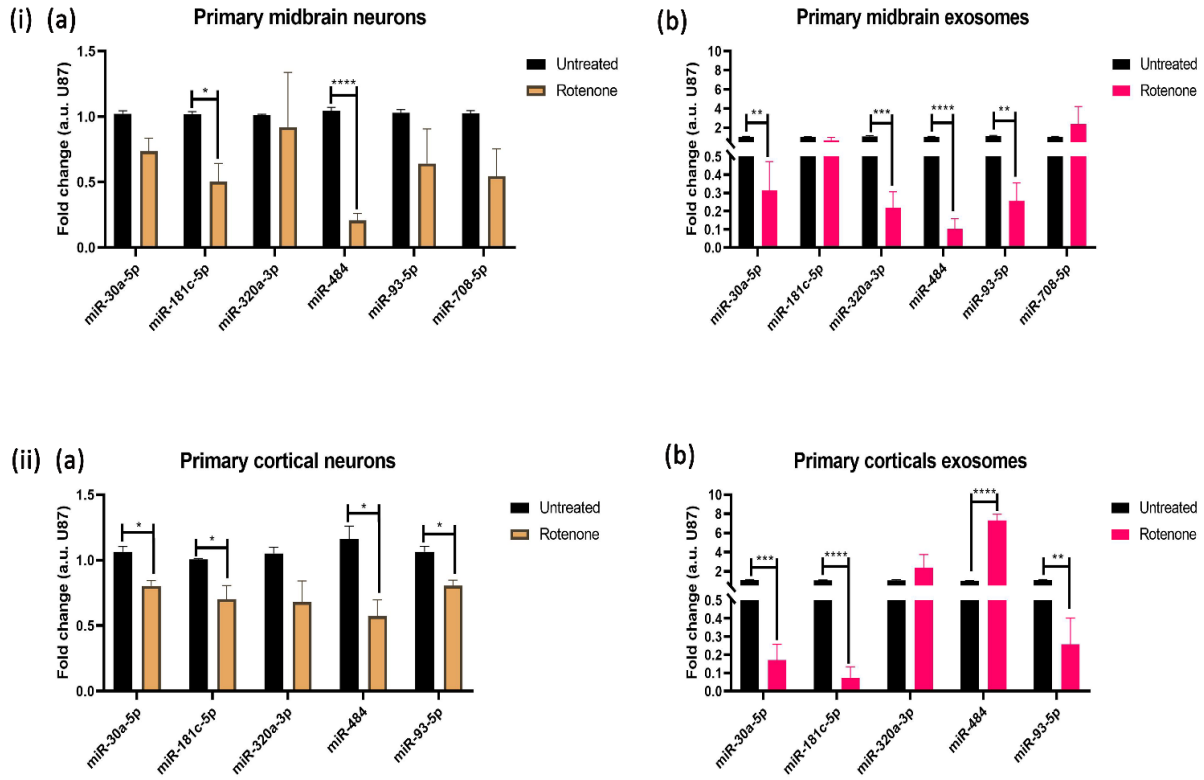


**Figure 4.3.5. Exosomal miRNA levels are altered in primary neuronal cells and exosomes on treatment with rotenone:** (i) Primary midbrain neurons and (ii) Primary cortical neurons were treated with 25nm and 60nm rotenone respectively for 24h and subsequently exosomes were isolated and differential expression of miRNAs were checked in (a) total cells and (b) exosomes by RT-qPCR. Asterisk (\*), (\*\*), (\*\*\*) and (\*\*\*\*) indicates values statistically significant from control; p value <0.05, <0.01, <0.001 and <0.0001 (respectively), SEM of three or four independent experiments, data was analyzed using one-way ANOVA, followed by Dunnett’s multiple comparisons test.

**4.3.4 Exosomes from serum and cerebrospinal fluid of acute rotenone-treated rats have differential expressions of miRNAs**

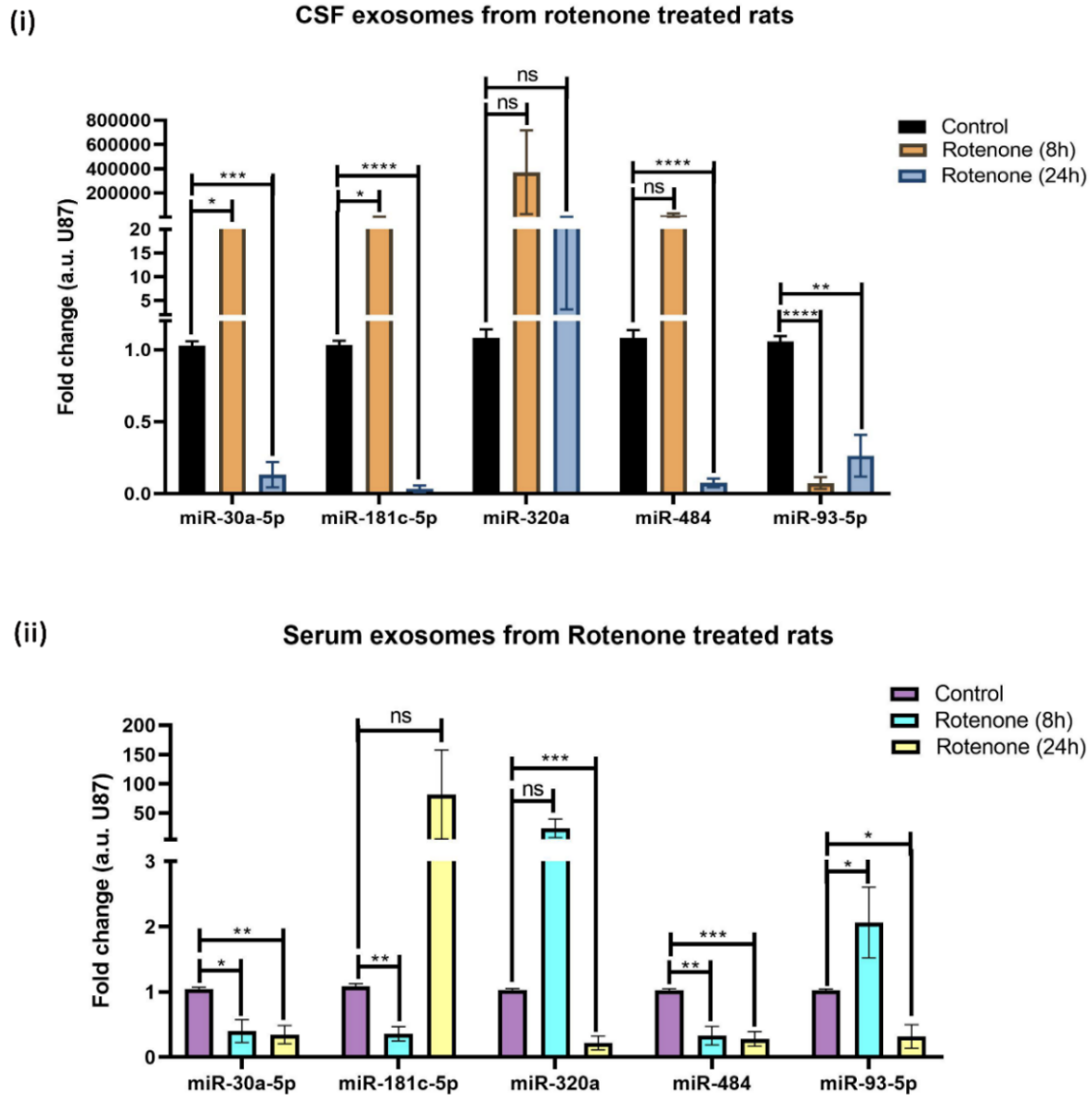


**Figure 4.3.6. Exosomal miRNAs are differentially expressed in biofluids of rotenone-treated rat models of PD:** Acute rotenone toxicity was administered to young adult male Sprague-Dawley rats of 3 months of age at a concentration of 3mg/kg for 8h and 24h. Biofluids were subsequently collected from the rats post-euthanasia and exosomes were isolated from the biofluids. The differential expression of exosomal miRNAs in the (i) cerebrospinal fluid (CSF) and (ii) serum were determined by RT-qPCR. Asterisk (\*), (\*\*), (\*\*\*) and (\*\*\*\*) indicates values

statistically significant from control; p value <0.05, <0.01, <0.001 and <0.0001 (respectively), SEM of ten independent experiments, data was analyzed using one-way ANOVA, followed by Dunnett's multiple comparisons test.

Further, exosomal miRNAs that were validated in the primary neuronal exosomes, were validated in the serum and CSF exosomes of acute rotenone-treated rats by qRT-PCR. The level of miR-181c-5p and miR-30a-5p increased in exosomes derived from CSF at 8h rotenone treatment, which later decreased significantly after 24h rotenone treatment. The levels of miR-93-5p are lower at both time points as compared to untreated rats (Fig 4.3.6(i)). Levels of both miR-30a-5p and miR-484 were downregulated at both time points of rotenone in serum exosomes as compared to the untreated serum exosomes. However, the levels of miR-181c-5p are low at 8h rotenone treatment, which increased at 24h rotenone treatment. However, the levels of miR-93-5p was high at 8h and decreased at 24h of rotenone treatment (Fig 4.3.6(ii)). The above results indicated that the exosomal miRNA levels are differentially sorted at early treatment time points of rotenone and is altered between 8h and 24h time points of treatment. Specific miRNAs showed consistent changes; level of miR-93-5p decreased in the exosomes from CSF and miR-30a-5p and miR-484 was decreased in exosomes from serum of rotenone treated rats.

### 4.3.5 Serum exosomes from acute rotenone-treated rats induce mitochondrial dysfunction and cell death in primary neurons from rat embryos

(i) Serum exosomes treated to primary midbrain neurons (ii) Serum exosomes treated to primary midbrain neurons



(iii) Serum exosomes treated to primary cortical neurons (iv) Serum exosomes treated to primary cortical neurons

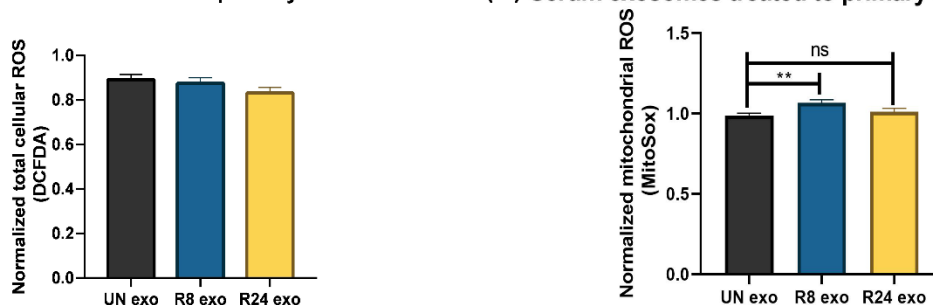


**Figure 4.3.7. Serum exosomes alter mitochondrial functions in primary neurons from rat embryos:** Serum exosomes derived from rotenone-treated rats were incubated with primary midbrain ((i) and (ii)) and cortical neurons and ((iii) and (iv)) and total cellular ROS was determined by DCFDA, and mitochondrial ROS was assessed using MitoSox staining. Asterisk (\*) and (\*\*) indicates values statistically significant from control; p value <0.05 and <0.01 (respectively), SEM of five independent experiments, data was analyzed using one-way ANOVA, followed by Dunnett's multiple comparisons test.

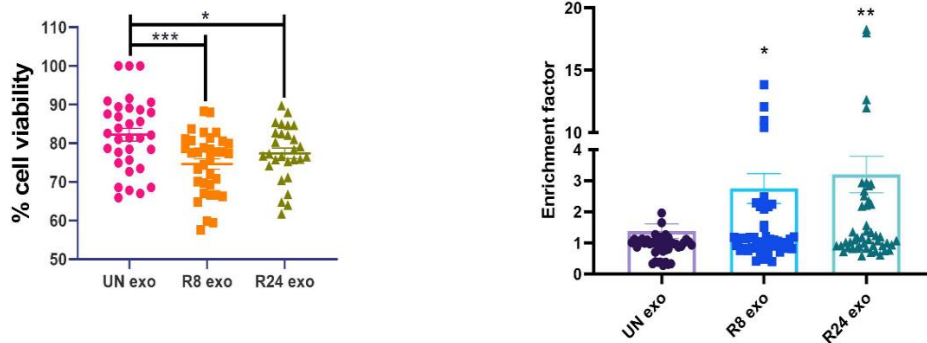
To study the effect of exosomes on primary neurons, serum exosomes isolated from healthy rats (referred to as UN exo) and the acute rotenone-treated rats of 8h (referred to as R8 exo) and of 24h (referred to as R24 exo) were incubated with primary midbrain and cortical neurons, and mitochondrial functions and cell viability was assessed. R8 exo significantly increased the total cellular ROS levels (Fig 4.3.7(i)) as well as mitochondrial specific ROS levels (Fig 4.3.7(ii)) in primary midbrain neurons as compared to the UN exo, while R24 exo showed no effect. The total

cellular ROS levels remained unaltered by the treatment of R8 and R24 exo to primary cortical neurons (Fig 4.3.7(iii)). However, R8 exo significantly increased the mitochondrial ROS levels in primary cortical neurons (Fig 4.3.7(iv)).

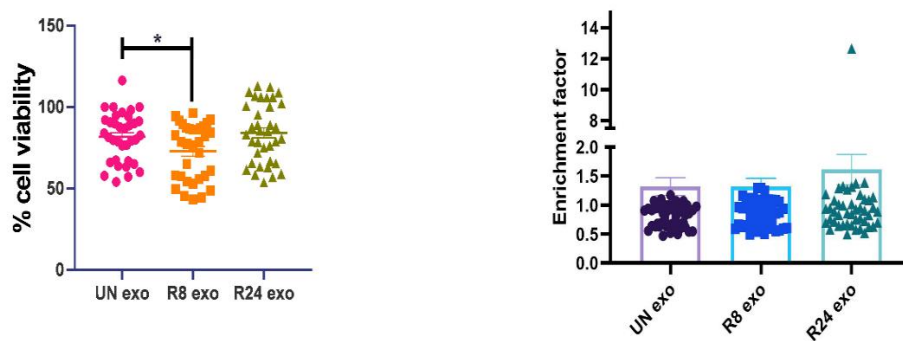
Primary midbrain neurons showed decreased cell viability on incubation with both R8 exo and R24 exo (Fig 4.3.8(i)(a)). Similar results were obtained by the cell death detection ELISA, where increased enrichment of mono- and oligonucleosomes is observed in the cytoplasm, which is indicative of apoptotic cells, in the presence of R8 exo and R24 exo (Fig 4.3.8(i)(b)). On contrary, primary cortical neurons were incubated with R8 exo showed cell death by MTT (Fig 4.3.8(ii)(a)). The ELISA did not show any significant enrichment of mono-/oligonucleosomes on incubation with serum exosomes (Fig 4.3.8(ii)(b)).

Since significant loss in cell viability was observed in primary midbrain neurons, analysis was done if serum exosomes exhibited a specific toxicity to the midbrain dopaminergic neurons. The ratio of TH neurons over MAP2 is significantly lower on incubation with R8 exo and R24 exo (Fig 4.3.8(iii)) suggesting that the dopaminergic neuron population specifically is affected by the treatment of serum exosomes.

(i) (a) Serum exosomes treated to primary midbrain neurons (b) Serum exosomes treated to primary midbrain neurons



(ii) (a) Serum exosomes treated to primary cortical neurons (b) Serum exosomes treated to primary cortical neurons



(iii) (a) UN exo R8 exo R24 exo (b) Serum exosomes treated to primary midbrain neurons

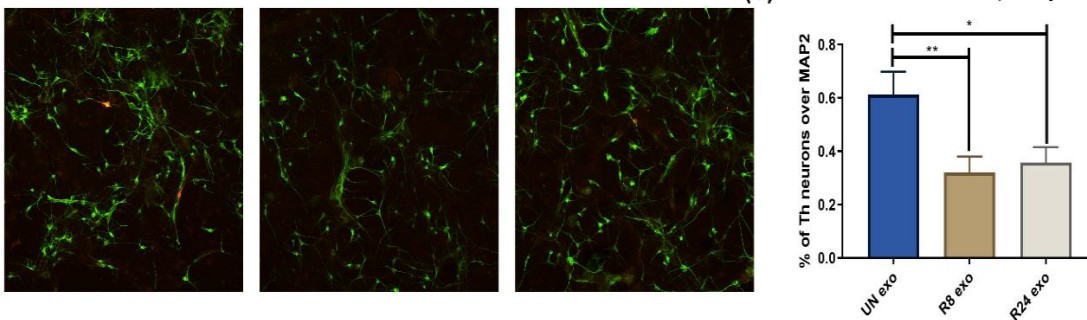
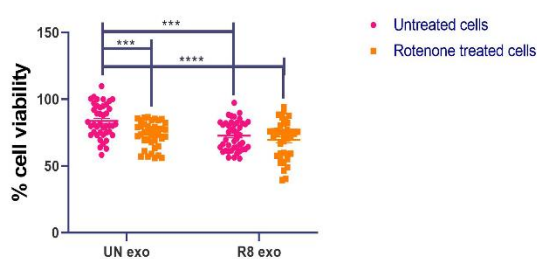


**Figure 4.3.8. Serum exosomes from acute rotenone-treated rat models of PD decreases the cell viability of primary neurons from rat embryos:** Serum exosomes from rotenone-treated rat models of PD at both 8h and 24h were incubated with primary neurons at a concentration of 50 $\mu$ g/mL. Post-treatment, the cell viability was assessed in (i) primary midbrain neurons and (ii) primary cortical neurons by using (a) MTT cell viability assay and (b) cell death detection by DNA damage ELISA. (iii) (a) Serum exosomes were treated to primary midbrain neurons as mentioned above, and the cells were fixed post-treatment and immunocytochemistry was performed in the cells using TH for specific dopaminergic neurons and MAP2 as a general neuronal marker, and the cells were observed using confocal microscopy and (b) % quantification of TH neurons over MAP2 was calculated by counting the cells using Nikon analysis software. A minimum of 10 fields per well were considered, analyzing over 200 cells per field. Asterisk (\*),

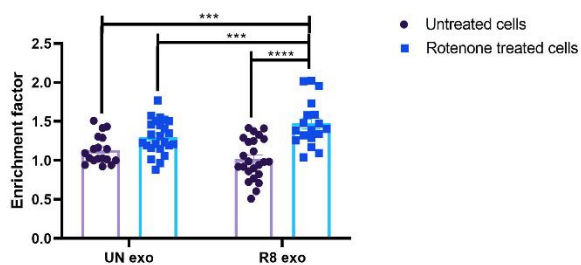
(\*\*) and (\*\*\*) indicates values statistically significant from control; p value <0.05, <0.01 and <0.001 (respectively), SEM of three and five independent experiments, data was analyzed using one-way ANOVA, followed by Dunnett's multiple comparisons test.

### 4.3.6 Serum exosomes exacerbate rotenone-induced dopaminergic neuron cell death in primary midbrain neurons from rat embryos

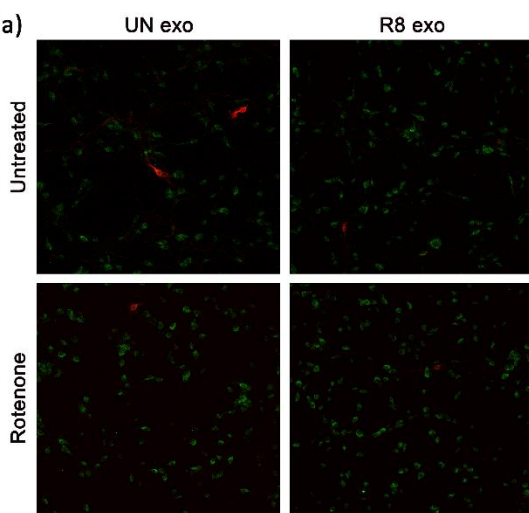
(i) Serum exosomes treated to primary midbrain neurons pre-treated with Rotenone



(ii) Serum exosomes treated to primary midbrain neurons pre-treated with Rotenone



(iii) (a)



(b)

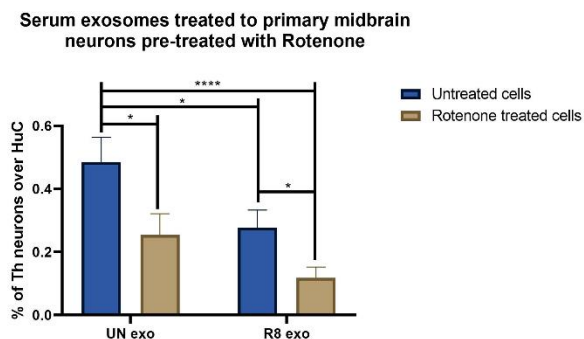


**Figure 4.3.9. R8 exo from serum of acute rotenone-treated rat models of PD exacerbates rotenone-induced cell death of primary midbrain neurons from rat embryos:** Serum exosomes from rotenone-treated rat models of PD at 8h were incubated with primary neurons pre-treated with 25nM rotenone at a concentration of 50µg/mL. Post-treatment, cell viability was assessed using (i) MTT cell viability assay and (ii) cell death detection by DNA damage ELISA. (iii) (a) Serum exosomes were treated to primary midbrain neurons as mentioned above, and the cells were fixed post-treatment and immunocytochemistry was performed in the cells using TH for specific dopaminergic neurons and HuC as a general neuronal marker, and the cells were observed using confocal microscopy and (b) %

quantification of TH neurons over HuC was calculated by counting the cells using Nikon analysis software. A minimum of 10 fields per well were considered, analyzing over 200 cells per field. Asterisk (\*), (\*\*\*) and (\*\*\*\*) indicates values statistically significant from control; p value <0.05, <0.001 and <0.0001 (respectively), SEM of three independent experiments, data was analyzed using one-way ANOVA, followed by Tukey's multiple comparisons test.

These data indicated that the serum exosomal cargo from rats treated with 8h of rotenone (R8 exo) induced mitochondrial dysfunction and cell death in primary midbrain neurons and specifically the dopaminergic neurons. Therefore, the effect of these exosomes on primary midbrain neurons which were already pre-treated with rotenone was done.

R8 exo was incubated with primary midbrain neurons that were pre-treated with 25nM of rotenone for 24h and the cell death was assessed by MTT cell viability staining. Significant loss in cell viability was obtained on treatment of rotenone and R8 exo to the cells alone. The cell death was exacerbated when the R8 exo and rotenone is co-treated to the primary midbrain neurons (Fig 4.3.9(i)). On performing the cell death detection by ELISA method, significant enrichment of mono-and oligonucleosomes was observed in the cells treated with both R8 exo and rotenone as compared to the individual treatments alone (Fig 4.3.9(ii)).

Further analysis was done whether the toxicity was specific to dopaminergic neurons of the midbrain. Dopaminergic neurons were tagged with TH (Tyrosine Hydroxylase), and a general neuronal marker, HuC, was used to tag the other neurons, and the ratio of TH-positive neurons over HuC was calculated for the above-mentioned treatment conditions (Fig 4.3.9(iii)(a)). There was a decrease in the ratio of Th neurons over HuC when cells were treated with rotenone of R8 exo alone, which was further reduced when these were treated together (Fig 4.3.9(iii)(b)).

### **4.3.7 Discussion**

The spread of pathogenesis from dopaminergic neurons to other regions of the brain during PD pathogenesis is not well understood. Exosomes have emerged as mediator of intercellular communication in different patho-physiological conditions however its role in the spread of pathogenesis; from dopaminergic neurons to other regions of the brain and other body fluids and have not been systemically investigated. Moreover, biomarkers for early detection of PD remain

lacking. To address this gap and advance understanding of mechanisms of PD progression, neurobiology of exosomes were explored in response to a well characterized PD relevant neurotoxin. Here, differentially expressed exosomal miRNAs were identified in response to an acute systemic PD model.

It has been previously reported that both genetic or sporadic cases exhibit abnormalities in the mitochondrial functions and pathways [336], [337]. Now it is known that pathogenesis of PD extends beyond the dopaminergic neurons of SN (substantia nigra) and exosomes may also contribute to this spread of pathogenesis. However, it is not known if mitochondrial dysfunction in dopaminergic neurons and neurons of other brain regions like cortex leads to any alteration in exosome release and changes in exosomal miRNA signatures. Rotenone was used as a model to induce mitochondrial dysfunction, which is a cardinal feature of PD and investigated exosome release and monitored its level in serum and CSF and explored neurotoxic potential. Previous study (previous chapter) indicated that PD stress (rotenone) can enhance the exosome release in neuroblastoma as well as glial cell lines. The exosome concentration that is released from primary midbrain and cortical neurons was analyzed, since midbrain region is particularly susceptible in PD and the latter, not so much, on exposure to acute rotenone toxicity. Exosome concentration is increased on rotenone treatment to primary neurons which is concordant with the previous results of the study (previous chapters). To understand the complexity of the heterogenous nature of these nanovesicles, various studies have attempted to isolate different subpopulations of exosomes with different biodistributions and functions [203], [338]. One group identified exosome subpopulations based on size by using asymmetric flow field-flow fractionation (AF4) technology [339]. Through NTA analysis, the extracellular vesicles were categorized (as mentioned in results section). While the large EVs and microvesicles made up most of the population of the vesicles, surprisingly there was no detection of 'exomere' population in the primary neurons, which are reported to be enriched in metabolic enzymes, and are involved in specific pathways, like glycolysis and mTOR signalling [339]. Interestingly, the total concentration of EVs microvesicle population increased significantly from primary neurons. A recent study demonstrated that the microvesicle population of EVs transfers active mitochondria from brain endothelial cells to recipient cells, elevating the ATP levels, indicating increased cell survival [340]. This study has demonstrated changes in the mitochondrial functions on treatment of exosomes, which supports the above report hinting at various cellular functions that might be affected in PD conditions.

The detection of PD presently is heavily reliant on clinical symptoms, which are not observed until the later stage of the disease. Detection at the earlier stage is essential, because at that time the drugs or disease-modifying compounds can show the highest therapeutic effect. Currently, there is no validated diagnostic biomarker for PD. To establish a clinically relevant biomarker, the use of body fluids is preferred, the collection of which would also be non-invasive or minimally invasive (e.g., CSF, blood, saliva, urine). The use of CSF was considered ideal for the detection of a biomarker, because of its proximity to the CNS [341]. However,  $\alpha$ -synuclein levels in blood or CSF can lack specificity [342], hence there is need to develop alternative biomarkers for the detection of PD. The circulating miRNAs in the body fluids then were beginning to be explored as promising biomarkers for PD [343], [344]. Exosomal miRNAs were examined in primary neurons on treatment with rotenone. Two miRNAs – hsa-miR-30a-5p and hsa-miR-181c-5p were significantly downregulated in both primary midbrain and cortical neurons, which recapitulates the results that were previously obtained in the *in vitro* model of PD in SH-SY5Y neuroblastoma cells (previous chapter).

Subsequently, examination of the circulating exosomal miRNAs in the biofluids of the acute rotenone rat models of PD was done to validate previous findings. NTA analysis of CSF exosomes of rats showed no significant changes, however serum exosomes were significantly elevated in rotenone treated rats. Unlike primary neurons, the CSF and serum exosome population showed presence of exomeres. Exo-S represent canonical exosomes, and Exo-L on the other hand are non-canonical exosomes/sEVs of different subcellular origin; both the types of EVs contain the miRNAs and other small RNA populations [339].

Validation of exosomal miRNAs revealed differential regulation at the different time points of rotenone treatment. A high variability in the levels of the miRNAs was observed at different time points. This suggests that miRNA changes under different acute conditions of rotenone is highly dynamic, which is in consonance with earlier studies [345], [346]. Exosomal miRNAs are dynamically regulated in response to acute exercise versus sustained exercise [345], as well as in response to different antitumor therapies (chemotherapy versus surgery) for lung cancer [346]. In this study miR-93-5p was consistently decreased in CSF-derived exosomes, and the steady low levels of miR-30a-5p and miR-484 in the serum of rotenone treated rats could serve as potential biomarkers for early stage of PD.

The CSF is separated from the rest of the peripheral body fluids by the presence of a selective physiological barrier, the blood-brain barrier (BBB). Interestingly, exosome transport through BBB has now been well-studied hence exosomal cargo from brain can be transferred to sites outside the brain giving rise to extra neuronal phenotype in PD [258], [347]. A study reported the presence of astrocyte-specific exosome protein cargo in the blood of rats, demonstrating the bidirectional movement of exosomes across BBB [348]. The miRNA changes observed here in the rotenone-rat model indicated that miR-181c-5p is significantly high in CSF where at 8h of rotenone treatment, but its levels in serum are low. Contrarily, at 24h of rotenone treatment, the miR-181c-5p levels drop significantly in the CSF and are elevated in the serum, which could be indicative of the bidirectional pathway of the exosomal cargo across the BBB.

Emerging reports suggest that exosomal miRNAs are vital in mediating mitochondrial functions and affect the mitochondrial activities in the cell, which is a distinct hallmark of PD [349]. Both R8 exo and R24 exo induced increased cellular ROS as well as mitochondrial-specific ROS in primary midbrain neurons. A similar study has shown that serum exosomes from PD mouse models contain elevated miR-137 levels which affects the oxidative stress in neurons [249]. Two independent studies have shown that microglial exosomes induced by LPS and  $\alpha$ -synuclein respectively, induce neuronal apoptosis leading to neurodegeneration [350], [351]. However, the effect of rotenone-induced serum exosomes had not been explored for their functional capabilities. On observing significant loss in cell viability due to treatment of serum exosomes, the current study confirmed that the cell death observed in the primary midbrain neurons is specific to the dopaminergic neuron population.

Moreover, apart from the effect of the exosomes on healthy primary midbrain neurons, the effect of these exosomes on neurons that are already sensitized to the neuronal insult (rotenone), is still elusive. Since, the R8 exosomal cargo was sufficient to induce mitochondrial alterations and cell death, the next part of the study was only performed with treatment of R8 exo to the primary midbrain neurons. Both the cell viability tests proved that the cell death was exacerbated in the treatment of R8 exo to the rotenone-induced primary midbrain neurons as compared to both the treatments individually. Further, the specific dopaminergic neurons in the midbrain were also decreased on treatment of R8 exo to rotenone-induced primary midbrain neurons, as compared to both treatments alone. In the context of PD, where the loss of dopaminergic neurons is a key

feature, these results suggest that the cargo is carried by the R8 exosomes might contribute to or accelerate the degeneration of dopaminergic neurons, particularly those already under stress from rotenone toxicity. In conclusion, this study showed the enhanced exosome release by rotenone-induced mitochondrial dysfunction from both primary and midbrain neurons as well as acute rotenone model of rat in vivo. Further specific miRNAs (like miR-93-5p is consistently downregulated in CSF, and the levels of miR-30a-5p and miR-484 were differentially present in the exosomes from primary and rat model) provides insight into the exploitation of exosomal miRNAs in biofluids as potential diagnostic/prognostic biomarkers for early detection of PD. Further, serum exosomes when treated to primary midbrain neurons displayed mitochondrial defects in terms of ROS generation, leading to neuronal cell death. This cell death was exacerbated when the recipient cells were pre-treated with rotenone along with receiving exosomes from the serum.